Numerische Mathematik (2020) 144:585–614
https://doi.org/10.1007/s00211-019-01095-x

Numerische Mathematik

Divergence-conforming discontinuous Galerkin finite elements for Stokes eigenvalue problems

Joscha Gedicke[1] · **Arbaz Khan**[2]

Received: 19 September 2018 / Revised: 16 September 2019 / Published online: 26 December 2019

Abstract
In this paper, we present a divergence-conforming discontinuous Galerkin finite element method for Stokes eigenvalue problems. We prove a priori error estimates for the eigenvalue and eigenfunction errors and present a residual based a posteriori error estimator. The a posteriori error estimator is proven to be reliable and (locally) efficient. We finally present some numerical examples that verify the a priori convergence rates and the reliability and efficiency of the residual based a posteriori error estimator.

Mathematics Subject Classification 65N15 · 65N25 · 65N30

1 Introduction

In fluid mechanics, eigenvalue problems are of great importance because of their role for the stability analysis of fluid flow problems. Hence, the development of numerical methods for the Stokes problem, as a model for incompressible fluid flow, is of great interest. For example in [22], several stabilized finite element methods for the Stokes eigenvalue problem are considered by Huang et al. A finite element analysis of a pseudo stress formulation for the Stokes eigenvalue problem is proposed by Meddahi et al. [33].

The first author has been funded by the Austrian Science Fund (FWF) through the Projects P 29197-N32 and M 2640-N32. The second author has been funded by the Mathematics Center Heidelberg (Match) at University of Heidelberg, Germany and EPSRC Grant EP/P013317.

✉ Arbaz Khan
arbaz.khan@manchester.ac.uk; arbazkha@gmail.com

Joscha Gedicke
gedicke@ins.uni-bonn.de

1 Institute for Numerical Simulation, University of Bonn, Endenicher Allee 19b, 53115 Bonn, Germany

2 Department of Mathematics, The University of Manchester, Manchester M13 9PL, UK

Currently, there are only very few results on the a posteriori error analysis for the Stokes eigenvalue problem available in the literature. An a posteriori error analysis based on residual a posteriori error estimators for the finite element discretization of the Stokes eigenvalue problem is proposed by Lovadina et al. [32]. Some superconvergence results and the related recovery type a posteriori error estimators for the Stokes eigenvalue problem is presented by Liu et al. [31] based on a projection method. In [2], Armentano et al. introduced a posteriori error estimators for stabilized low-order mixed finite elements and in [19], Han et al. presented a residual type a posterior error estimator for a new adaptive mixed finite element method for the Stokes eigenvalue problem. In [21], Huang presents a posteriori lower and upper eigenvalue bounds for the Stokes eigenvalue problem for two stabilized finite element methods based on the lowest equal-order finite element pair. Recently, we have developed an a posteriori error analysis for the Arnold-Winther mixed finite element method of the Stokes eigenvalue problem in [16] using the stress-velocity formulation.

Cockburn et al. [13,14] derived the divergence-conforming discontinuous Galerkin finite element method. In [20], Houston et al. presented an a posteriori error estimation for mixed discontinuous Galerkin approximations of the Stokes problem. Kanschat et al. [26] proposed a posteriori error estimates for divergence-free discontinuous Galerkin approximations of the Navier-Stokes equations. Multigrid methods for H^{div}-conforming discontinuous Galerkin (H^{div}-DG) finite element methods for the Stokes equations are proposed by Kanschat et al. [25]. Recently, Kanschat et al. [27] presented the relation between the H^{div}-DG finite element method for the Stokes equation and the C^0 interior penalty finite element method for the biharmonic problem.

In this paper, we introduce an H^{div}-DG finite element method for Stokes eigenvalue problems. We derive a priori error estimates for the eigenvalue and eigenfunction errors. We present a residual based a posteriori error analysis for the H^{div}-DG finite element method and derive upper and local lower bounds for the eigenvalue error and the velocity-pressure error which is measured in terms of the mesh-dependent DG norm.

For traditional mixed methods, the lack of divergence-conforming approximations introduces a pressure-dependent consistency error which dominates the velocity error for small velocity parameters when the right hand side is not divergence-free. In that case additional stabilization is needed. For an overview of different stabilization techniques for weakly divergence-free mixed methods and a comprehensive discussion on the issue of pressure robustness can be found in [23]. Moreover, for small velocity parameters and non divergence-free right hand sides, the standard residual a posteriori error estimator for the source problem is dominated by the estimation of the pressure error. In that situation a more efficient a posteriori error estimator for the velocity error can be obtained from exploiting stream-functions. For the H^{div}-DG finite element method such a refined a posteriori error estimator has been introduced in [27, sec. 4.1] and for classical mixed (stabilized) finite element methods recently in [29]. Note that for the eigenvalue problem the right hand side is always divergence-free and therefore the eigenvalue problem does not suffer from small viscosity parameters and any stable approximation of any eigenfunctions is pressure-robust. Hence, the refined a posteriori error analysis which requires more smootheness of the right hand side than L^2 and which involves the calculation of third order derivatives for higher order methods is not needed for the eigenvalue problem, and one can rely on simpler to implement a posteriori error estimators involving the pressure without loosing robustness.

For simplicity of the presentation we restrict the analysis to the case of a simple eigenvalue λ. The results can be applied to multiple eigenvalues by extending the given analysis to subspaces of eigenvectors that belong to the same multiple eigenvalue. The a posteriori error estimator can be extended to multiple eigenvalues in that the squared sum over all estimators of discrete eigenfunctions approximating the same multiple eigenvalue provides an upper bound of the eigenvalue error up to higher order terms, see also [8].

The paper is organised as follows: the necessary notation and the H^{div}-DG formulation of the Stokes eigenvalue problem is presented in Sect. 2. In Sect. 3, the a priori error analysis is discussed. The a posteriori error analysis is developed in Sect. 4. Finally, Sect. 5 is devoted to present some numerical results for uniform and adaptive mesh refinement.

2 Preliminaries

2.1 Notation

Define $\boldsymbol{u} = (u_1, u_2)^t \in \mathbb{R}^2$, $\boldsymbol{v} = (v_1, v_2)^t \in \mathbb{R}^2$, $\boldsymbol{\sigma} = (\sigma_{ij})_{2\times 2}$, and $\boldsymbol{\tau} = (\tau_{ij})_{2\times 2}$, then

$$\nabla \boldsymbol{v} = \begin{pmatrix} \frac{\partial v_1}{\partial x_1} & \frac{\partial v_1}{\partial x_2} \\ \frac{\partial v_2}{\partial x_1} & \frac{\partial v_2}{\partial x_2} \end{pmatrix}, \qquad \nabla \cdot \boldsymbol{v} = \frac{\partial v_1}{\partial x_1} + \frac{\partial v_2}{\partial x_2}, \qquad \boldsymbol{u} \otimes \boldsymbol{v} = \begin{pmatrix} u_1 v_1 & u_1 v_2 \\ u_2 v_1 & u_2 v_2 \end{pmatrix},$$

$$\operatorname{div}(\boldsymbol{\tau}) = \begin{pmatrix} \frac{\partial \tau_{11}}{\partial x_1} + \frac{\partial \tau_{12}}{\partial x_2} \\ \frac{\partial \tau_{21}}{\partial x_1} + \frac{\partial \tau_{22}}{\partial x_2} \end{pmatrix}, \qquad \text{and} \qquad \boldsymbol{\sigma} : \boldsymbol{\tau} = \sum_{j,k=1}^{2} \boldsymbol{\sigma}_{jk} \boldsymbol{\tau}_{jk}.$$

Let $H^s(\omega)$ be the standard Sobolev space with the associated norm $\|\cdot\|_{s,\omega}$ for an integer $s \geq 0$. In case of $\omega = \Omega$, we use $\|\cdot\|_s$ instead of $\|\cdot\|_{s,\Omega}$. Now we extend the definitions to vector and matrix-valued functions. Let $\boldsymbol{H}^s(\omega) = \boldsymbol{H}^s(\omega; \mathbb{R}^2)$ and $\boldsymbol{H}^s(\omega, \mathbb{R}^{2\times 2})$ be the Sobolev spaces over the set of 2-dimensional vector and 2×2 matrix-valued function, respectively. The symbols $\lesssim$ and $\gtrsim$ are used to denote bounds which are valid up to positive constants independent of the local mesh size and the (constant) viscosity parameter.

Throughout the paper, we consider the following spaces $L_0^2(\Omega)$, $\boldsymbol{H}^{\text{div}}(\Omega)$, $\boldsymbol{H}_0^{\text{div}}(\Omega)$ and $\boldsymbol{H}^{\text{div}}(\Omega, \mathbb{R}^{2\times 2})$ which are defined as follows:

$$L_0^2(\Omega) := \left\{ v \in L^2(\Omega) \mid \int_\Omega v \, dx = 0 \right\},$$
$$\boldsymbol{H}^{\text{div}}(\Omega) := \{ \boldsymbol{v} \in \boldsymbol{L}^2(\Omega) \mid \nabla \cdot \boldsymbol{v} \in L^2(\Omega) \},$$

$$\boldsymbol{H}_0^{\text{div}}(\Omega) := \{\boldsymbol{v} \in \boldsymbol{H}^{\text{div}}(\Omega) \mid \boldsymbol{v} \cdot \boldsymbol{n} = 0 \ \text{ on } \ \partial\Omega\},$$
$$\boldsymbol{H}^{\text{div}}(\Omega, \mathbb{R}^{2\times 2}) := \{\boldsymbol{\tau} \in \boldsymbol{L}^2(\Omega; \mathbb{R}^{2\times 2}) \mid \operatorname{div}(\boldsymbol{\tau}) \in \boldsymbol{L}^2(\Omega)\}.$$

2.2 Weak formulation of the Stokes eigenvalue problem

Let $\boldsymbol{u}$ be the velocity, p the pressure, $\nu > 0$ the (constant) viscosity, and $\Omega \subset \mathbb{R}^2$ be a bounded, and connected Lipschitz domain. Consider the velocity-pressure formulation of the Stokes eigenvalue problem: find an eigenpair $(\boldsymbol{u}, p, \lambda)$, $\boldsymbol{u} \neq \boldsymbol{0}$, such that

$$\begin{aligned} -\nu \triangle \boldsymbol{u} + \nabla p &= \lambda \boldsymbol{u} && \text{in } \Omega, \\ \nabla \cdot \boldsymbol{u} &= 0 && \text{in } \Omega, \\ \boldsymbol{u} &= \boldsymbol{0} && \text{on } \partial\Omega, \end{aligned} \tag{1}$$

with the compatibility relation

$$\int_\Omega p \, dx = 0.$$

The weak formulation of the Stokes eigenvalue problem (1) reads: find $(\boldsymbol{u}, p, \lambda) \in \boldsymbol{H}_0^1(\Omega) \times L_0^2(\Omega) \times \mathbb{R}_+$ such that $\|\boldsymbol{u}\|_0 = 1$ and

$$\begin{aligned} \nu(\nabla \boldsymbol{u}, \nabla \boldsymbol{v}) - (p, \nabla \cdot \boldsymbol{v}) &= \lambda(\boldsymbol{u}, \boldsymbol{v}) && \forall \boldsymbol{v} \in \boldsymbol{H}_0^1(\Omega), \\ (q, \nabla \cdot \boldsymbol{u}) &= 0 && \forall q \in L_0^2(\Omega). \end{aligned} \tag{2}$$

We can formulate the weak formulation of (2) on the product space as: find $(\boldsymbol{u}, p, \lambda) \in \boldsymbol{H}_0^1(\Omega) \times L_0^2(\Omega) \times \mathbb{R}_+$ such that $\|\boldsymbol{u}\|_0 = 1$ and

$$\mathscr{A}(\boldsymbol{u}, p; \boldsymbol{v}, q) = \lambda(\boldsymbol{u}, \boldsymbol{v}) \quad \forall (\boldsymbol{v}, q) \in \boldsymbol{H}_0^1(\Omega) \times L_0^2(\Omega), \tag{3}$$

where

$$\mathscr{A}(\boldsymbol{u}, p; \boldsymbol{v}, q) = \nu(\nabla \boldsymbol{u}, \nabla \boldsymbol{v}) - (p, \nabla \cdot \boldsymbol{v}) - (q, \nabla \cdot \boldsymbol{u}).$$

2.3 Meshes, trace operators and discrete spaces

We suppose that the domain Ω is decomposed by a subdivision $\mathscr{T}_h$ into a mesh of shape-regular rectangular cells K. Let $\mathscr{E}_h$ denote the set of edges, $\mathscr{E}_h^i$ the set of interior edges, and $\mathscr{E}_h^\partial$ the set of boundary edges of $\mathscr{T}_h$. We restrict ourselves to one-irregular meshes $\mathscr{T}_h$ in which each interior edge $E \in \mathscr{E}_h^i$ may contain at most one hanging node in the midpoint of E.

For a given mesh $\mathscr{T}_h$, the notions of broken spaces for the continuous and differentiable function spaces are denoted as $C^0(\mathscr{T}_h)$ and $H^s(\mathscr{T}_h)$ which are the spaces such that the restriction to each mesh cell $K \in \mathscr{T}_h$ is in $C^0(K)$ and $H^s(K)$, respectively.

Let $K_\pm \in \mathscr{T}_h$ be two mesh cells which share a common edge $E = K_+ \cap K_- \in \mathscr{E}_h^i$. The traces of functions $v \in C^0(\mathscr{T}_h)$ on E from $K_\pm$ are defined as $v_\pm$, respectively. Then the sum operator is defined as

$$[\![v]\!] = v_+ + v_-.$$

Let $\boldsymbol{n}_\pm$ be the unit outward normal vector to $K_\pm$, respectively. Then the sum operator turns into the jump operator, such that for $\boldsymbol{v} \in C^1(\mathscr{T}_h; \mathbb{R}^2)$

$$[\![\partial \boldsymbol{v}/\partial \boldsymbol{n}]\!] = \nabla(\boldsymbol{v}_+ - \boldsymbol{v}_-)\boldsymbol{n}_+, \quad \text{and} \quad [\![\boldsymbol{v} \otimes \boldsymbol{n}]\!] = (\boldsymbol{v}_+ - \boldsymbol{v}_-) \otimes \boldsymbol{n}_+.$$

For boundary edges $E = K_+ \cap \partial\Omega$ we set $[\![\boldsymbol{v}]\!] = \boldsymbol{v}_+$ and with ∇_h we denote the local application of the gradient $(\nabla_h \boldsymbol{v})|_K = \nabla(\boldsymbol{v}|_K)$ on each $K \in \mathscr{T}_h$.

We define $Q_k(K)$, $Q_k(K)^d$ and $Q_k(K)^{d\times d}$ as the space of scalar, vector and tensor valued polynomials on K of partial degree at most integer $k \geq 1$.

Choose $\boldsymbol{V}_h$ as a discrete subspace of $\boldsymbol{H}_0^{\text{div}}(\Omega)$ as

$$\boldsymbol{V}_h = \{\boldsymbol{v} \in \boldsymbol{H}_0^{\text{div}}(\Omega) \mid \forall K \in \mathscr{T}_h : \boldsymbol{v}|_K \in RT_k(K) \text{ for } k \geq 1\}, \tag{4}$$

where $RT_k(K) := \mathscr{P}_{k+1,k}(K) \times \mathscr{P}_{k,k+1}(K)$ is the Raviart–Thomas space of degree $k \geq 1$, where $\mathscr{P}_{r,s}(K)$ denotes the space of the polynomial functions on K of degree at most $r > 0$ in x_1 and at most $s > 0$ in x_2. Moreover, let Q_h be the discrete space of $L_0^2(\Omega)$ such that

$$Q_h = \{v \in L_0^2(\Omega) \mid \forall K \in \mathscr{T}_h : v|_K \in Q_k(K) \text{ for } k \geq 1\}. \tag{5}$$

An important property of the pair $\boldsymbol{V}_h \times Q_h$ is as follows: on the meshes considered,

$$\nabla \cdot \boldsymbol{V}_h \subset Q_h,$$

see [13] for more details. As a consequence we have that the discrete velocity field $\boldsymbol{u}_h$ is exactly divergence free.

Remark 1 Here, we recall remark 2.1 of [26], that the inf-sup stability of RT_k/Q_k finite element discretizations with more than one-irregular hanging nodes or $k = 1$ is still an open question. It has been conjectured in [26] that stability also holds for $k = 1$ and one-irregular hanging nodes, which is computationally verified by our numerical experiments of Sect. 5. The following results are all to be read in view of these restrictions.

Remark 2 The analysis of this paper also applies directly to divergence-free BDM_k/P_{k-1} finite elements [11,12] on regular triangular meshes.

2.4 H^{div}-DG formulation for the Stokes eigenvalue problem

The discrete weak formulation of problem (1) reads: find $(\boldsymbol{u}_h, p_h, \lambda_h) \in \boldsymbol{V}_h \times Q_h \times \mathbb{R}_+$ such that $\|\boldsymbol{u}_h\|_0 = 1$ and

$$\mathscr{A}_h(\boldsymbol{u}_h, p_h; \boldsymbol{v}_h, q_h) = \lambda_h(\boldsymbol{u}_h, \boldsymbol{v}_h) \quad \forall(\boldsymbol{v}_h, q_h) \in \boldsymbol{V}_h \times Q_h, \tag{6}$$

where

$$\mathscr{A}_h(\boldsymbol{u}_h, p_h; \boldsymbol{v}_h, q_h) = a_h(\boldsymbol{u}_h, \boldsymbol{v}_h) - (p_h, \nabla \cdot \boldsymbol{v}_h) - (q_h, \nabla \cdot \boldsymbol{u}_h).$$

Here, $a_h(\cdot, \cdot)$ is the bilinear form defined as

$$\begin{aligned} a_h(\boldsymbol{u}, \boldsymbol{v}) &= \nu(\nabla_h \boldsymbol{u}, \nabla_h \boldsymbol{v}) + a_h^i(\boldsymbol{u}, \boldsymbol{v}) + a_h^\partial(\boldsymbol{u}, \boldsymbol{v}), \\ a_h^i(\boldsymbol{u}, \boldsymbol{v}) &= a_p^i(\boldsymbol{u}, \boldsymbol{v}) - a_c^i(\boldsymbol{u}, \boldsymbol{v}) - a_c^i(\boldsymbol{v}, \boldsymbol{u}), \\ a_h^\partial(\boldsymbol{u}, \boldsymbol{v}) &= a_p^\partial(\boldsymbol{u}, \boldsymbol{v}) - a_c^\partial(\boldsymbol{u}, \boldsymbol{v}) - a_c^\partial(\boldsymbol{v}, \boldsymbol{u}), \end{aligned}$$

where the interior face terms $a_p^i(\boldsymbol{u}, \boldsymbol{v})$, $a_c^i(\boldsymbol{u}, \boldsymbol{v})$ and Nitsche terms are defined as

$$a_c^i(\boldsymbol{u}, \boldsymbol{v}) = \frac{\nu}{2} \sum_{E \in \mathscr{E}_h^i} \int_E [\![\nabla_h \boldsymbol{u}]\!] : [\![\boldsymbol{v} \otimes \boldsymbol{n}]\!] ds, \quad a_p^i(\boldsymbol{u}, \boldsymbol{v}) = \nu \sum_{E \in \mathscr{E}_h^i} \int_E \gamma_h [\![\boldsymbol{u} \otimes \boldsymbol{n}]\!] : [\![\boldsymbol{v} \otimes \boldsymbol{n}]\!] ds,$$

$$a_c^\partial(\boldsymbol{u}, \boldsymbol{v}) = \nu \sum_{E \in \mathscr{E}_h^\partial} \int_E \nabla \boldsymbol{u} : (\boldsymbol{v} \otimes \boldsymbol{n}) ds, \qquad a_p^\partial(\boldsymbol{u}, \boldsymbol{v}) = 2\nu \sum_{E \in \mathscr{E}_h^\partial} \int_E \gamma_h (\boldsymbol{u} \otimes \boldsymbol{n}) : (\boldsymbol{v} \otimes \boldsymbol{n}) ds,$$

for $\gamma_h = \frac{\gamma}{h_E}$, and $\boldsymbol{u}, \boldsymbol{v} \in \boldsymbol{V}_h$. Here, h_E is the length of the edge E and γ is the penalty parameter which is chosen sufficiently large to guarantee the stability of the DG formulation, see for instance [3].

Finally, we introduce the following mesh-dependent DG velocity-pressure norm

$$|||(\boldsymbol{u}, p)|||^2 = |||\boldsymbol{u}|||^2 + \nu^{-1} \|p\|_0^2, \tag{7}$$

where

$$|||\boldsymbol{u}|||^2 = \nu \|\nabla_h \boldsymbol{u}\|_0^2 + a_p^i(\boldsymbol{u}, \boldsymbol{u}) + a_p^\partial(\boldsymbol{u}, \boldsymbol{u}).$$

Remark 3 We observe that the DG norm (7) is well balanced in ν for continuous/discrete eigenfunctions. This is due to the fact that for constant velocity, the velocity eigenfunctions do not change in ν and thus the eigenvalues as well as the pressure eigenfunctions scale linearly in ν, i.e. the eigenpair for arbitrary (constant) ν is $(\boldsymbol{u}, \nu p, \nu\lambda)$, where $(\boldsymbol{u}, p, \lambda)$ denotes the eigenpair for $\nu = 1$. Since the H^{div}-DG method is divergence-conforming, we deduce from (6) that the same scaling is also true in the discrete case. Hence, (7) is also well balanced in ν for the eigenfunction errors. (In the case of the source problem with non divergence-free right hand side,

(7) might not be well balanced and lead to a large overestimation of the velocity error by the DG velocity-pressure norm.)

3 A priori error analysis

Our main aim is to show that the approximated eigenvalues and eigenfunctions of the H^{div}-DG finite element formulation of the Stokes eigenvalue problem converge to the solution of the corresponding spectral problem which comes to apply the classical spectral approximation theory for mixed problems presented in [4,7,34] using results of the a priori error analysis of the associated source problem that we recall here for completeness.

3.1 Numerical analysis of the source problem

This section is devoted to discuss the source problem and to recall its essential stability and convergence results.

Consider the source problem with the right hand side $\boldsymbol{f} \in \boldsymbol{L}^2(\Omega)$

$$\begin{aligned} -\nu \triangle \boldsymbol{u}^{\boldsymbol{f}} + \nabla p^{\boldsymbol{f}} &= \boldsymbol{f} \quad \text{in } \Omega, \\ \nabla \cdot \boldsymbol{u}^{\boldsymbol{f}} &= 0 \quad \text{in } \Omega, \\ \boldsymbol{u}^{\boldsymbol{f}} &= 0 \quad \text{on } \partial\Omega, \end{aligned}$$

with compatibility condition

$$\int_\Omega p^{\boldsymbol{f}}\, dx = 0.$$

The variational formulation of the Stokes source problem reads: find $(\boldsymbol{u}^{\boldsymbol{f}}, p^{\boldsymbol{f}}) \in \boldsymbol{H}_0^1(\Omega) \times L_0^2(\Omega)$ such that

$$\mathscr{A}(\boldsymbol{u}^{\boldsymbol{f}}, p^{\boldsymbol{f}}; \boldsymbol{v}, q) = (\boldsymbol{f}, \boldsymbol{v}) \quad \forall (\boldsymbol{v}, q) \in \boldsymbol{H}_0^1(\Omega) \times L_0^2(\Omega). \tag{8}$$

Due to the continuous inf-sup condition

$$\inf_{0 \neq q \in L_0^2(\Omega)} \sup_{\mathbf{0} \neq \boldsymbol{v} \in \boldsymbol{H}_0^1(\Omega)} \frac{-(q, \nabla \cdot \boldsymbol{v})}{\|\nabla \boldsymbol{v}\|_0 \|q\|_0} > 0, \tag{9}$$

the variational formulation (8) is well-posed [12,18].

The H^{div}-DG finite element formulation of the Stokes source problem reads: find $(\boldsymbol{u}_h^{\boldsymbol{f}}, p_h^{\boldsymbol{f}}) \in \boldsymbol{V}_h \times Q_h$ such that

$$\mathscr{A}_h(\boldsymbol{u}_h^{\boldsymbol{f}}, p_h^{\boldsymbol{f}}; \boldsymbol{v}_h, q_h) = (\boldsymbol{f}, \boldsymbol{v}_h) \quad \forall (\boldsymbol{v}_h, q_h) \in \boldsymbol{V}_h \times Q_h. \tag{10}$$

From [14,26,27], we have that the bilinear form $a_h(\cdot,\cdot)$ is bounded and elliptic uniformly in h on $\boldsymbol{V}_h$ equipped with the norm $|||\cdot|||$. Furthermore, the velocity-pressure pair $\boldsymbol{V}_h \times Q_h$ is inf-sup stable and satisfies

$$\inf_{0\neq q_h\in Q_h} \sup_{\boldsymbol{0}\neq \boldsymbol{v}_h\in \boldsymbol{V}_h} \frac{-(q_h, \nabla\cdot\boldsymbol{v}_h)}{|||\boldsymbol{v}_h|||\,\|q_h\|_0} \geq \beta > 0,$$

for a constant β independent of h. Hence, the weak formulation (10) has a unique discrete solution, which admits the following stability estimate

$$\left|\left|\left|(\boldsymbol{u}_h^{\boldsymbol{f}}, p_h^{\boldsymbol{f}})\right|\right|\right| \lesssim \nu^{-1/2}\|\boldsymbol{f}\|_0,$$

and due to $\nabla\cdot\boldsymbol{V}_h \subset Q_h$ the discrete velocity $\boldsymbol{u}_h^{\boldsymbol{f}}$ is exactly divergence-free.

From [17, Section 3] and [23, Section 4.4], we have the following a priori estimates.

Theorem 1 *Let $\boldsymbol{u}^{\boldsymbol{f}} \in \boldsymbol{H}^s(\Omega)$ and $p^{\boldsymbol{f}} \in H^{s-1}(\Omega)$ for some $s \in]3/2, k+1]$ be solutions of the continuous problem* (8) *that satisfy the following stability condition, cf.* [28, Theorem 1] *along with* [23, Lemma 2.8],

$$\nu^{1/2}\|\boldsymbol{u}^{\boldsymbol{f}}\|_s + \nu^{-1/2}\|p^{\boldsymbol{f}}\|_{s-1} \lesssim \begin{cases} \nu^{-1/2}\|\boldsymbol{f}\|_0, & s\in(\frac{3}{2},2), \\ \nu^{-1/2}\|\boldsymbol{f}\|_{s-2}, & s\geq 2. \end{cases} \tag{11}$$

Then we have the following error bounds for the discrete approximations $(\boldsymbol{u}_h, p_h) \in \boldsymbol{V}_h \times Q_h$ of the discrete problem (10)

$$\left|\left|\left|\boldsymbol{u}^{\boldsymbol{f}} - \boldsymbol{u}_h^{\boldsymbol{f}}\right|\right|\right| \lesssim h^{s-1}(\nu^{1/2}\|\boldsymbol{u}^{\boldsymbol{f}}\|_s), \tag{12}$$

$$\nu^{-1/2}\|p^{\boldsymbol{f}} - p_h^{\boldsymbol{f}}\|_0 \lesssim h^{s-1}(\nu^{1/2}\|\boldsymbol{u}^{\boldsymbol{f}}\|_s + \nu^{-1/2}\|p^{\boldsymbol{f}}\|_{s-1}), \tag{13}$$

$$\|\boldsymbol{u}^{\boldsymbol{f}} - \boldsymbol{u}_h^{\boldsymbol{f}}\|_0 \lesssim h^{s-1+\alpha}\|\boldsymbol{u}^{\boldsymbol{f}}\|_s, \tag{14}$$

for $\alpha = \min\{s-1, 1\}$.

3.2 Numerical analysis of the eigenvalue problem

We now derive the convergence of eigenvalues and eigenfunctions of the discrete problem (6) to those of the continuous problem (3) and estimate the order of convergence. Since the solution operator to the mixed problem (3) is not compact, we cannot apply the standard Babuška-Osborn theory [4] directly. Therefore, we utilize the theory for mixed eigenvalue problems from Mercier et. al. [34], cf. also [4,7], by introducing separate solution operators for the velocity and pressure components.

Using the well posedness of the continuous source problem (8), the operators $T : \boldsymbol{L}^2(\Omega) \to \boldsymbol{H}_0^1(\Omega)$ and $S : \boldsymbol{L}^2(\Omega) \to L_0^2(\Omega)$ are well defined for any $\boldsymbol{f} \in \boldsymbol{L}^2(\Omega)$ such that $T\boldsymbol{f} = \boldsymbol{u}^{\boldsymbol{f}}$ and $S\boldsymbol{f} = p^{\boldsymbol{f}}$ are the velocity and pressure components of the solution to problem (8).

For given $\boldsymbol{f} \in \boldsymbol{L}^2(\Omega)$, $(T\boldsymbol{f}, S\boldsymbol{f}) \in \boldsymbol{H}_0^1(\Omega) \times L_0^2(\Omega)$ is the solution of

$$\mathscr{A}(T\boldsymbol{f}, S\boldsymbol{f}; \boldsymbol{v}, q) = (\boldsymbol{f}, \boldsymbol{v}) \quad \forall(\boldsymbol{v}, q) \in \boldsymbol{H}_0^1(\Omega) \times L_0^2(\Omega). \tag{15}$$

Since the discrete source problem (10) is well posed, we define in the same manner the operators $T_h : \boldsymbol{L}^2(\Omega) \to \boldsymbol{V}_h$ and $S_h : \boldsymbol{L}^2(\Omega) \to Q_h$ such that $T_h\boldsymbol{f} = \boldsymbol{u}_h^{\boldsymbol{f}}$ and $S_h\boldsymbol{f} = p_h^{\boldsymbol{f}}$ are the discrete velocity and the discrete pressure approximations. The H^{div}-DG finite element formulation of the Stokes source problem becomes the following: find $(T_h\boldsymbol{f}, S_h\boldsymbol{f}) \in \boldsymbol{V}_h \times Q_h$ such that

$$\mathscr{A}_h(T_h\boldsymbol{f}, S_h\boldsymbol{f}; \boldsymbol{v}, q) = (\boldsymbol{f}, \boldsymbol{v}) \quad \forall(\boldsymbol{v}, q) \in \boldsymbol{V}_h \times Q_h. \tag{16}$$

Moreover, we deduce the following estimates from Theorem 1

$$|||T\boldsymbol{f} - T_h\boldsymbol{f}||| \lesssim h^{s-1}(\nu^{1/2}\|\boldsymbol{u}^{\boldsymbol{f}}\|_s), \tag{17}$$

$$\nu^{-1/2}\|S\boldsymbol{f} - S_h\boldsymbol{f}\|_0 \lesssim h^{s-1}(\nu^{1/2}\|\boldsymbol{u}^{\boldsymbol{f}}\|_s + \nu^{-1/2}\|p^{\boldsymbol{f}}\|_{s-1}), \tag{18}$$

$$\|T\boldsymbol{f} - T_h\boldsymbol{f}\|_0 \lesssim h^{s-1+\alpha}\|\boldsymbol{u}^{\boldsymbol{f}}\|_s, \tag{19}$$

for $\alpha = \min\{s-1, 1\}$.

Note that the operator T_h is well defined in $\boldsymbol{L}^2(\Omega)$ but not in $\boldsymbol{H}_0^1(\Omega)$. Hence, we can only conclude convergence of the operators T_h in $\boldsymbol{L}^2(\Omega)$ from the abstract theory. From (18), (19), and the satbility (11) we conclude

$$\|T - T_h\|_{\mathscr{L}(\boldsymbol{L}^2(\Omega), \boldsymbol{L}^2(\Omega))} \lesssim \nu^{-1}h^{s-1+\alpha}, \tag{20}$$

$$\|S - S_h\|_{\mathscr{L}(\boldsymbol{L}^2(\Omega), L_0^2(\Omega))} \lesssim h^{s-1}. \tag{21}$$

Note that the eigenvalues λ are the reciprocal values of the eigenvalues of the operator T. To see that, let

$$\boldsymbol{H}(\Omega) := \{\boldsymbol{v} \in \boldsymbol{L}^2(\Omega) \mid \operatorname{div}(\boldsymbol{v}) = 0, \ \gamma_\nu(\boldsymbol{v}) = 0\},$$

where γ_ν denotes the normal trace operator. Then T considered from $\boldsymbol{H}(\Omega)$ to $\boldsymbol{H}(\Omega)$ is the inverse of the Stokes operator as defined in [9, Section IV.5.2]. Hence, from [9, Section II.6.2] we conclude that T is bounded, compact, and self adjoint from $\boldsymbol{H}(\Omega)$ to $\boldsymbol{H}(\Omega)$, and we can apply the spectral theory for compact operators. Therefore, the eigenvalues form an increasing sequence of positive real numbers which tends to infinity and, since $\boldsymbol{u} \neq \boldsymbol{0}$, we get from (2) that $\nu(\nabla\boldsymbol{u}, \nabla\boldsymbol{u})/(\boldsymbol{u}, \boldsymbol{u}) = \lambda > 0$, cf. also [9, Theorem IV.5.5].

Theorem 2 *Let $(\boldsymbol{u}, p, \lambda) \in \boldsymbol{H}^s(\Omega) \times H^{s-1}(\Omega) \times \mathbb{R}^+$ for some $s \in]3/2, k+1]$ be a solution of the continuous eigenvalue problem (1), then the following estimate holds*

$$|\lambda - \lambda_h| \lesssim (\lambda_h\lambda^{-1})\left(\nu + h^{2\alpha}\|\nabla\boldsymbol{u}\|_0^2\right)h^{2(s-1)}\|\boldsymbol{u}\|_s^2 \tag{22}$$

for $\alpha = \min\{s-1, 1\}$.

Proof Since T and T_h are compact on $\boldsymbol{H}(\Omega)$ we can apply the Babuška-Osborn theory, i.e. [7, theorem 9.7] with $\mathscr{X} = \boldsymbol{H}(\Omega)$ and multiplicity $\alpha = 1$. Therefore

$$\begin{aligned}|\lambda^{-1} - \lambda_h^{-1}| &\lesssim |((T - T_h)\boldsymbol{u}, \boldsymbol{u}^*)| \\ &\quad + \|(T - T_h)_{|E}\|_{\mathscr{L}(\boldsymbol{H}(\Omega);\boldsymbol{H}(\Omega))} \|(T^* - T_h^*)_{|E^*}\|_{\mathscr{L}(\boldsymbol{H}(\Omega);\boldsymbol{H}(\Omega))}.\end{aligned}$$

Since T and T_h are self adjoint, we have $T^* = T$ and $T_h^* = T_h$. Hence, we have

$$\frac{|\lambda - \lambda_h|}{\lambda\lambda_h} = |\lambda^{-1} - \lambda_h^{-1}| \lesssim |((T - T_h)\boldsymbol{u}, \boldsymbol{u})| + \|(T - T_h)_{|E}\|^2_{\mathscr{L}(\boldsymbol{H}(\Omega);\boldsymbol{H}(\Omega))}. \tag{23}$$

The second term of (23) is directly estimated by (20). To estimate the first term of (23), we use the weak formulations (15) and (16), and consistency of $\mathscr{A}_h$ [38, Lemma 7.5], to deduce

$$\begin{aligned}&\mathscr{A}_h(T\boldsymbol{u} - T_h\boldsymbol{u}, S\boldsymbol{u} - S_h\boldsymbol{u}; T\boldsymbol{u} - T_h\boldsymbol{u}, S\boldsymbol{u} - S_h\boldsymbol{u}) \\ &\quad = \mathscr{A}(T\boldsymbol{u}, S\boldsymbol{u}; T\boldsymbol{u}, S\boldsymbol{u}) + \mathscr{A}_h(T_h\boldsymbol{u}, S_h\boldsymbol{u}; T_h\boldsymbol{u}, S_h\boldsymbol{u}) - 2\mathscr{A}_h(T\boldsymbol{u}, S\boldsymbol{u}; T_h\boldsymbol{u}, S_h\boldsymbol{u}) \\ &\quad = (\boldsymbol{u}, T\boldsymbol{u}) + (\boldsymbol{u}, T_h\boldsymbol{u}) - 2(\boldsymbol{u}, T_h\boldsymbol{u}) = ((T - T_h)\boldsymbol{u}, \boldsymbol{u}).\end{aligned} \tag{24}$$

Note that the velocity $T\boldsymbol{u}$ and the discrete velocity $T_h\boldsymbol{u}$ are divergence free. Therefore we have

$$\begin{aligned}((T - T_h)\boldsymbol{u}, \boldsymbol{u}) &= \mathscr{A}_h(T\boldsymbol{u} - T_h\boldsymbol{u}, S\boldsymbol{u} - S_h\boldsymbol{u}; T\boldsymbol{u} - T_h\boldsymbol{u}, S\boldsymbol{u} - S_h\boldsymbol{u}), \\ &= a_h(T\boldsymbol{u} - T_h\boldsymbol{u}, T\boldsymbol{u} - T_h\boldsymbol{u}).\end{aligned} \tag{25}$$

From the continuity of $a_h(\cdot, \cdot)$, we get

$$a_h(T\boldsymbol{u} - T_h\boldsymbol{u}, T\boldsymbol{u} - T_h\boldsymbol{u}) \lesssim |||T\boldsymbol{u} - T_h\boldsymbol{u}|||^2. \tag{26}$$

Combining (25)–(26) with $T\boldsymbol{u} = \lambda^{-1}\boldsymbol{u}$, and $\nu^{-1} = \|\nabla\boldsymbol{u}\|_0^2/\lambda$ in (23) in combination with (17) gives the desired result. □

From the Babuška-Osborn theory [7, Theorem 9.3] we get the following rates of convergence for the $\boldsymbol{L}^2(\Omega)$ error for the velocity component $\boldsymbol{u}$ under the regularity conditions from Theorem 2

$$\|\boldsymbol{u} - \boldsymbol{u}_h\|_0 \lesssim \|(T - T_h)_{|E}\|_{\mathscr{L}(\boldsymbol{H}(\Omega);\boldsymbol{H}(\Omega))} \lesssim \nu^{-1}h^{s-1+\alpha}, \tag{27}$$

for $s \in]3/2, k+1]$, and $\alpha = \min\{s-1, 1\}$.

For the $L^2(\Omega)$ error for the pressure component p of the eigenfunctions we get from the triangle inequality, the stability (11), and the estimates (21), (22), and (27), that

$$\begin{aligned}\|p - p_h\|_0 &= \|S(\lambda \boldsymbol{u}) - S_h(\lambda_h \boldsymbol{u}_h)\|_0 \\ &\leq \|S(\lambda \boldsymbol{u} - \lambda_h \boldsymbol{u}_h)\|_0 + \|(S - S_h)(\lambda_h \boldsymbol{u}_h)\|_0 \\ &\lesssim \|\lambda \boldsymbol{u} - \lambda_h \boldsymbol{u}_h\|_0 + \|(S - S_h)(\lambda_h \boldsymbol{u}_h)\|_0 \\ &\lesssim h^{s-1}\left(\lambda_h + h^{\alpha}\|\nabla \boldsymbol{u}\|_0^2 + (\lambda_h \lambda^{-1})(\nu + h^{2\alpha}\|\nabla \boldsymbol{u}\|_0^2)h^{s-1}\|u\|_s^2\right).\end{aligned} \tag{28}$$

Theorem 3 *The following estimate holds for* $s \in]3/2, k+1]$

$$\begin{aligned}&|||\boldsymbol{u} - \boldsymbol{u}_h||| \\ &\quad\lesssim (\lambda_h \lambda^{-1})h^{s-1}\left(\nu^{1/2}\|\boldsymbol{u}\|_s + h^{\alpha}\|\nabla \boldsymbol{u}\|_0^2 + \lambda^{-1/2}\left(\nu + h^{2\alpha}\|\nabla \boldsymbol{u}\|_0^2\right)h^{2(s-1)}\|\boldsymbol{u}\|_s^2\right).\end{aligned}$$

Proof Let λ be the eigenvalue corresponding to the eigenfunction $\boldsymbol{u}$. Then it holds that

$$\boldsymbol{u} - \boldsymbol{u}_h = \lambda T\boldsymbol{u} - \lambda_h T_h \boldsymbol{u}_h = (\lambda - \lambda_h)T\boldsymbol{u} + \lambda_h(T - T_h)\boldsymbol{u} + \lambda_h T_h(\boldsymbol{u} - \boldsymbol{u}_h).$$

It follows that

$$|||\boldsymbol{u} - \boldsymbol{u}_h||| \lesssim \nu^{1/2}\lambda^{-1}|\lambda - \lambda_h|\|\nabla \boldsymbol{u}\|_0 + \lambda_h|||(T - T_h)\boldsymbol{u}||| + \lambda_h|||T_h(\boldsymbol{u} - \boldsymbol{u}_h)|||.$$

The first two terms of the right hand side are directly estimated by (22) and (12), and the last term is estimated using (10) as follows

$$\begin{aligned}|||T_h(\boldsymbol{u} - \boldsymbol{u}_h)|||^2 &\lesssim \mathscr{A}_h(T_h(\boldsymbol{u} - \boldsymbol{u}_h), S_h(\boldsymbol{u} - \boldsymbol{u}_h); T_h(\boldsymbol{u} - \boldsymbol{u}_h), S_h(\boldsymbol{u} - \boldsymbol{u}_h)) \\ &= ((\boldsymbol{u} - \boldsymbol{u}_h), T_h(\boldsymbol{u} - \boldsymbol{u}_h)).\end{aligned}$$

Applying Cauchy–Schwarz inequality and (27), implies

$$|||T_h(\boldsymbol{u} - \boldsymbol{u}_h)||| \lesssim \|\boldsymbol{u} - \boldsymbol{u}_h\|_0 \lesssim \nu^{-1}h^{s-1+\alpha},$$

where $\alpha = \min\{s-1, 1\}$. Using $\nu^{-1} = \|\nabla \boldsymbol{u}\|_0^2/\lambda$, and $\lambda^{1/2} = \nu^{1/2}\|\nabla \boldsymbol{u}\|_0$ finishes the proof. □

We will now establish a relationship between the eigenvalue and the eigenfunction errors. In order to do so, we observe that the numerical scheme is consistent.

Lemma 1 *Let* $(\boldsymbol{u}, p, \lambda) \in \boldsymbol{H}_0^1(\Omega) \times L_0^2(\Omega) \times \mathbb{R}_+$ *be the solution of* (3). *If* $\boldsymbol{u} \in \boldsymbol{H}^2(\mathscr{T}_h)$ *and* $p \in H^1(\mathscr{T}_h)$, *then*

$$\mathscr{A}_h(\boldsymbol{u}, p; \boldsymbol{v}_h, q_h) = \lambda(\boldsymbol{u}, \boldsymbol{v}_h) \quad \forall(\boldsymbol{v}_h, q_h) \in \boldsymbol{V}_h \times Q_h.$$

Proof The result follows from the consistency of the discontinuous Galerkin finite element method for the source problem [38, Lemma 7.5]. □

Theorem 4 *Let* $(\boldsymbol{u}, p, \lambda) \in \boldsymbol{H}_0^1(\Omega) \times L_0^2(\Omega) \times \mathbb{R}_+$ *be the solution of* (3) *and* $(\boldsymbol{u}_h, p_h) \in \boldsymbol{V}_h \times Q_h$ *with* $\|\boldsymbol{u}_h\|_0 \neq 0$. *If* $\boldsymbol{u} \in \boldsymbol{H}^2(\mathscr{T}_h)$ *and* $p \in H^1(\mathscr{T}_h)$, *then the Rayleigh quotient satisfies the following identity*

$$\frac{\mathscr{A}_h(\boldsymbol{u}_h, p_h; \boldsymbol{u}_h, p_h)}{\|\boldsymbol{u}_h\|_0^2} - \lambda = \frac{\mathscr{A}_h(\boldsymbol{u} - \boldsymbol{u}_h, p - p_h; \boldsymbol{u} - \boldsymbol{u}_h, p - p_h)}{\|\boldsymbol{u}_h\|_0^2} - \lambda \frac{\|\boldsymbol{u} - \boldsymbol{u}_h\|_0^2}{\|\boldsymbol{u}_h\|_0^2}.$$

Proof Note that

$$\mathscr{A}_h(\boldsymbol{u}, p; \boldsymbol{u}, p) = \mathscr{A}(\boldsymbol{u}, p; \boldsymbol{u}, p) \quad \forall\, (\boldsymbol{u}, p) \in \boldsymbol{H}_0^1(\Omega) \times L_0^2(\Omega).$$

Moreover, from consistency we get

$$\begin{aligned} &\mathscr{A}_h(\boldsymbol{u} - \boldsymbol{u}_h, p - p_h; \boldsymbol{u} - \boldsymbol{u}_h, p - p_h) \\ &\quad = \mathscr{A}(\boldsymbol{u}, p; \boldsymbol{u}, p) + \mathscr{A}_h(\boldsymbol{u}_h, p_h; \boldsymbol{u}_h, p_h) - 2\mathscr{A}_h(\boldsymbol{u}, p; \boldsymbol{u}_h, p_h) \\ &\quad = \lambda(\boldsymbol{u}, \boldsymbol{u}) + \mathscr{A}_h(\boldsymbol{u}_h, p_h; \boldsymbol{u}_h, p_h) - 2\lambda(\boldsymbol{u}, \boldsymbol{u}_h). \end{aligned} \tag{29}$$

Next we write the following identity

$$\lambda(\boldsymbol{u} - \boldsymbol{u}_h, \boldsymbol{u} - \boldsymbol{u}_h) = \lambda(\boldsymbol{u}, \boldsymbol{u}) + \lambda(\boldsymbol{u}_h, \boldsymbol{u}_h) - 2\lambda(\boldsymbol{u}, \boldsymbol{u}_h). \tag{30}$$

Subtracting (30) from (29), we obtain

$$\begin{aligned} &\mathscr{A}_h(\boldsymbol{u} - \boldsymbol{u}_h, p - p_h; \boldsymbol{u} - \boldsymbol{u}_h, p - p_h) - \lambda(\boldsymbol{u} - \boldsymbol{u}_h, \boldsymbol{u} - \boldsymbol{u}_h) \\ &\quad = \mathscr{A}_h(\boldsymbol{u}_h, p_h; \boldsymbol{u}_h, p_h) - \lambda(\boldsymbol{u}_h, \boldsymbol{u}_h). \end{aligned}$$

Dividing by $(\boldsymbol{u}_h, \boldsymbol{u}_h)$ on both sides in the above equation ends the proof. □

4 A posteriori error analysis

In this section, we present a residual based a posteriori error estimator for the Stokes eigenvalue problem.

Let $(\boldsymbol{u}_h, p_h, \lambda_h) \in \boldsymbol{V}_h \times Q_h \times \mathbb{R}_+$ be an eigenpair approximation. For each $K \in \mathscr{T}_h$, the interior residual estimator η_{R_K} is defined by

$$\eta_{R_K}^2 := \nu^{-1} h_K^2 \|\lambda_h \boldsymbol{u}_h + \nu \Delta \boldsymbol{u}_h - \nabla p_h\|_{0,K}^2,$$

and the edge residual estimator η_{E_K} by

$$\eta_{E_K}^2 := \nu^{-1} \sum_{E \in \partial K \setminus \partial\Omega} h_E \|[\![(p_h \boldsymbol{I} - \nu \nabla \boldsymbol{u}_h)\boldsymbol{n}]\!]\|_{0,E}^2,$$

where $\boldsymbol{I}$ denotes the 2×2 identity matrix. Next, we introduce the estimator η_{J_K}, which measures the jump of the approximate solution $\boldsymbol{u}_h$,

$$\eta_{J_K}^2 := \nu \sum_{E \in \partial K} \gamma_h \| [\![\boldsymbol{u}_h \otimes \boldsymbol{n}]\!] \|_{0,E}^2,$$

with $\gamma_h = \frac{\gamma}{h_E}$, where γ is the penalty parameter discussed in Sect. 2.4.
The local error indicator, which is the sum of the above three terms, is defined as

$$\eta_K^2 := \eta_{R_K}^2 + \eta_{E_K}^2 + \eta_{J_K}^2.$$

Finally, we introduce the (global) a posteriori error estimator

$$\eta_h := \left(\sum_{K \in \mathscr{T}_h} \eta_K^2 \right)^{1/2}. \tag{31}$$

4.1 Additional stability property

In the proof of reliability we will use the following auxiliary stability property following [20, Lemma 4.3], [26, Section 2.3]. We include the proof for the H^{div}-DG formulation of the Stokes problem for completeness.

Lemma 2 *For any $(\boldsymbol{u}, p) \in \boldsymbol{H}_0^1(\Omega) \times L_0^2(\Omega)$, there exists a pair $(\boldsymbol{v}, q) \in \boldsymbol{H}_0^1(\Omega) \backslash \{0\} \times L_0^2(\Omega)$ with $|\!|\!|(\boldsymbol{v}, q)|\!|\!| \lesssim |\!|\!|(\boldsymbol{u}, p)|\!|\!|$ and*

$$\mathscr{A}_h(\boldsymbol{u}, p; \boldsymbol{v}, q) \gtrsim |\!|\!|(\boldsymbol{u}, p)|\!|\!|^2.$$

Proof From the continuous inf-sup condition (9) we deduce that there exists a $\boldsymbol{w} \in \boldsymbol{H}_0^1(\Omega)$ such that

$$-(p, \nabla \cdot \boldsymbol{w}) \geq C_\Omega \nu^{-1} \|p\|_0^2, \qquad \text{and} \qquad \nu^{1/2} \|\nabla \boldsymbol{w}\|_0 \leq \nu^{-1/2} \|p\|_0,$$

where $C_\Omega > 0$ is the continuous inf-sup constant, which only depends on Ω. If $(\boldsymbol{u}, p) \in \boldsymbol{H}_0^1(\Omega) \times L_0^2(\Omega)$, then it holds that

$$\mathscr{A}_h(\boldsymbol{u}, p; \boldsymbol{u}, -p) = |\!|\!|\boldsymbol{u}|\!|\!|^2. \tag{32}$$

Moreover, using $\nu^{1/2} \|\nabla \boldsymbol{w}\|_0 \leq \nu^{-1/2} \|p\|_0$, continuity and Youngs inequality we get

$$\begin{aligned} \mathscr{A}_h(\boldsymbol{u}, p; \boldsymbol{w}, 0) &\geq C_\Omega \nu^{-1} \|p\|_0^2 - C |\!|\!|\boldsymbol{u}|\!|\!| \; |\!|\!|\boldsymbol{w}|\!|\!| \\ &\geq C_\Omega \nu^{-1} \|p\|_0^2 - \nu^{-1/2} C |\!|\!|\boldsymbol{u}|\!|\!| \; \|p\|_0 \\ &\geq \left(C_\Omega - \frac{1}{\epsilon} \right) \nu^{-1} \|p\|_0^2 - \epsilon C^2 |\!|\!|\boldsymbol{u}|\!|\!|^2, \end{aligned} \tag{33}$$

for a positive generic continuity constant $C > 0$. Using equations (32) and (33), we have

$$\begin{aligned}\mathscr{A}_h(\boldsymbol{u}, p; \boldsymbol{u} + \delta \boldsymbol{w}, -p) &= \mathscr{A}_h(\boldsymbol{u}, p; \boldsymbol{u}, -p) + \delta \mathscr{A}_h(\boldsymbol{u}, p; \boldsymbol{w}, 0)\\ &\geq |||\boldsymbol{u}|||^2 + \delta\left(C_\Omega - \frac{1}{\epsilon}\right)\nu^{-1}\|p\|_0^2 - \delta\epsilon C^2 |||\boldsymbol{u}|||^2\\ &\geq (1 - \delta\epsilon C^2)|||\boldsymbol{u}|||^2 + \delta\left(C_\Omega - \frac{1}{\epsilon}\right)\nu^{-1}\|p\|_0^2.\end{aligned}$$

Taking $\epsilon = 2/C_\Omega$ and $\delta = C_\Omega/(4C^2)$, it follows

$$\mathscr{A}_h(\boldsymbol{u}, p; \boldsymbol{u} + \delta \boldsymbol{w}, -p) \geq \min\left\{\frac{1}{2}, \frac{C_\Omega^2}{8C^2}\right\}|||(\boldsymbol{u}, p)|||^2. \tag{34}$$

Moreover, from $\nu^{1/2}\|\nabla \boldsymbol{w}\|_0 \leq \nu^{-1/2}\|p\|_0$ we get

$$\begin{aligned}|||(\boldsymbol{u} + \delta\boldsymbol{w}, -p)|||^2 &\leq 2|||\boldsymbol{u}|||^2 + 2\delta^2\nu\|\nabla\boldsymbol{w}\|_0^2 + \nu^{-1}\|p\|_0^2\\ &\leq \max\left\{2, \left(1 + \frac{C_\Omega^2}{8C^4}\right)\right\}|||(\boldsymbol{u}, p)|||^2.\end{aligned} \tag{35}$$

Combining equations (34) and (35), proves the final assertion with $\boldsymbol{v} = \boldsymbol{u} + \delta\boldsymbol{w}$ and $q = -p$. □

4.2 Reliability

First we define the discontinuous RT_k space $\widetilde{\boldsymbol{V}}_h = \{\boldsymbol{v} \in \boldsymbol{L}^2 : \boldsymbol{v}|_K \in RT_k(K),\ K \in \mathscr{T}_h\}$. As in [20,26], we define $\boldsymbol{V}_h^c = \widetilde{\boldsymbol{V}}_h \cap \boldsymbol{H}_0^1(\Omega)$. The orthogonal complement of $\boldsymbol{V}_h^c$ in $\widetilde{\boldsymbol{V}}_h$ with respect to the norm $|||\cdot|||$ is defined by $\boldsymbol{V}_h^\perp$. Then we obtain $\widetilde{\boldsymbol{V}}_h = \boldsymbol{V}_h^c \oplus \boldsymbol{V}_h^\perp$. Hence, we decompose the DG velocity approximation uniquely into

$$\boldsymbol{u}_h = \boldsymbol{u}_h^c + \boldsymbol{u}_h^r,$$

where $\boldsymbol{u}_h^c \in \boldsymbol{V}_h^c$ and $\boldsymbol{u}_h^r \in \boldsymbol{V}_h^\perp$. Using the triangle inequality, we can write

$$|||\boldsymbol{u} - \boldsymbol{u}_h||| \leq \left|\left|\left|\boldsymbol{u} - \boldsymbol{u}_h^c\right|\right|\right| + \left|\left|\left|\boldsymbol{u}_h^r\right|\right|\right|,$$

and from [20, Proposition 4.1] we get the upper bound for the second term

$$\left|\left|\left|\boldsymbol{u}_h^r\right|\right|\right| \lesssim \Big(\sum_{K\in\mathscr{T}_h} \eta_{J_K}^2\Big)^{1/2}. \tag{36}$$

Note that the DG bilinearform $a_h(\boldsymbol{u}, \boldsymbol{v})$ is not well defined for functions $\boldsymbol{u}, \boldsymbol{v}$ which belong to $\boldsymbol{H}_0^1(\Omega)$. One can overcome this difficulty by the use of a suitable lifting operator, cf. [14,26]. Here, we discuss a different approach where the DG form $a_h(\cdot,\cdot)$ is split into several parts,

$$a_h(\boldsymbol{u},\boldsymbol{v}) = \nu(\nabla_h \boldsymbol{u}, \nabla_h \boldsymbol{v}) + C_h(\boldsymbol{u},\boldsymbol{v}) + J_h(\boldsymbol{u},\boldsymbol{v}), \tag{37}$$

with

$$\begin{aligned} C_h(\boldsymbol{u},\boldsymbol{v}) &= -a_c^i(\boldsymbol{u},\boldsymbol{v}) - a_c^i(\boldsymbol{v},\boldsymbol{u}) - a_c^\partial(\boldsymbol{u},\boldsymbol{v}) - a_c^\partial(\boldsymbol{v},\boldsymbol{u}), \\ J_h(\boldsymbol{u},\boldsymbol{v}) &= a_p^i(\boldsymbol{u},\boldsymbol{v}) + a_p^\partial(\boldsymbol{v},\boldsymbol{u}). \end{aligned} \tag{38}$$

Lemma 3 *Let $\boldsymbol{u}_h \in \boldsymbol{V}_h$ and $\boldsymbol{v}_h^c \in \boldsymbol{V}_h^c$, then it holds that*

$$C_h(\boldsymbol{u}_h, \boldsymbol{v}_h^c) \lesssim \gamma^{-1/2}\Big(\sum_{K\in\mathscr{T}_h} \eta_{J_K}^2\Big)^{1/2} |||\boldsymbol{v}_h^c|||.$$

Proof Since $\boldsymbol{v}_h^c \in \boldsymbol{V}_h^c$, we have

$$C_h(\boldsymbol{u}_h, \boldsymbol{v}_h^c) = -a_c^i(\boldsymbol{v}_h^c, \boldsymbol{u}_h) - a_c^\partial(\boldsymbol{v}_h^c, \boldsymbol{u}_h).$$

Applying Cauchy–Schwarz inequality, implies

$$C_h(\boldsymbol{u}_h, \boldsymbol{v}_h^c) \lesssim \Big(\nu \sum_{E\in\mathscr{E}_h} \gamma_h^{-1} \|[\![\nabla \boldsymbol{v}_h^c]\!]\|_{0,E}^2\Big)^{1/2} \Big(\nu \sum_{E\in\mathscr{E}_h} \gamma_h \|[\![\boldsymbol{u}_h \otimes \boldsymbol{n}]\!]\|_{0,E}^2\Big)^{1/2}.$$

Using a trace estimate together with a discrete inverse inequality leads for an edge $E \in \mathscr{E}_h$, with $E = K_1 \cap K_2$ if $E \in \mathscr{E}_h^i$ and $E = K_1$, $K_2 = \emptyset$ if $E \subset \partial\Omega$, to

$$\|\nabla \boldsymbol{v}_h^c\|_{0,E} \lesssim h_K^{-1/2} \|\nabla \boldsymbol{v}_h^c\|_{0,K_1\cup K_2}.$$

Thus we have

$$C_h(\boldsymbol{u}_h, \boldsymbol{v}_h^c) \lesssim \gamma^{-1/2}\Big(\nu \sum_{K\in\mathscr{T}_h} \|\nabla \boldsymbol{v}_h^c\|_{0,K}^2\Big)^{1/2} \Big(\sum_{K\in\mathscr{T}_h} \eta_{J_K}^2\Big)^{1/2}.$$

□

Let $\boldsymbol{\Pi}_h : \boldsymbol{H}_0^1 \to \boldsymbol{V}_h^c$ denote the Scott–Zhang interpolation operator, which is stable $\|\nabla(\boldsymbol{\Pi}_h \boldsymbol{v})\|_0 \lesssim \|\nabla \boldsymbol{v}\|_0$ and satisfies the following interpolation property

$$\sum_{K\in\mathscr{T}_h} h_K^{-2} \|\boldsymbol{v} - \boldsymbol{\Pi}_h \boldsymbol{v}\|_{0,K}^2 + \sum_{E\in\mathscr{E}_h} h_E^{-1} \|\boldsymbol{v} - \boldsymbol{\Pi}_h \boldsymbol{v}\|_{0,E}^2 \lesssim \|\nabla \boldsymbol{v}\|_0^2, \tag{39}$$

for any $\boldsymbol{v} \in \boldsymbol{H}_0^1(\Omega)$, cf. [36, Corollary 4.1 & Theorem 4.1] for triangles and [18, Section A.2] for quadrilaterals. For edges with hanging nodes, as noted in [26, proof of Lemma 4.2], we take the interpolant from the unrefined edge to maintain conformity.

Lemma 4 *Let $\boldsymbol{v}_h^c = \boldsymbol{\Pi}_h \boldsymbol{v} \in \boldsymbol{V}_h^c$ be the Scott–Zhang interpolation of $\boldsymbol{v} \in \boldsymbol{H}_0^1(\Omega)$, then for any $\boldsymbol{u}_h \in \boldsymbol{V}_h$, $p_h \in Q_h$, and $\lambda_h \in \mathbb{R}_+$, it holds that*

$$\lambda_h(\boldsymbol{u}_h, \boldsymbol{v} - \boldsymbol{v}_h^c) - \nu(\nabla_h \boldsymbol{u}_h, \nabla(\boldsymbol{v} - \boldsymbol{v}_h^c)) + (p_h, \nabla \cdot (\boldsymbol{v} - \boldsymbol{v}_h^c)) \lesssim \eta_h |||\boldsymbol{v}|||.$$

Proof Using integration by parts on each element $K \in \mathscr{T}_h$, we have

$$\begin{aligned}
&\lambda_h(\boldsymbol{u}_h, \boldsymbol{v} - \boldsymbol{v}_h^c) - \nu(\nabla_h \boldsymbol{u}_h, \nabla(\boldsymbol{v} - \boldsymbol{v}_h^c)) + (p_h, \nabla \cdot (\boldsymbol{v} - \boldsymbol{v}_h^c)) \\
&= \sum_{K \in \mathscr{T}_h} \int_K (\lambda_h \boldsymbol{u}_h + \nu \Delta \boldsymbol{u}_h - \nabla p_h)(\boldsymbol{v} - \boldsymbol{v}_h^c) d\boldsymbol{x} \\
&\quad + \sum_{K \in \mathscr{T}_h} \int_{\partial K} (p_h \boldsymbol{I} - \nu \nabla \boldsymbol{u}_h)\boldsymbol{n}_K \cdot (\boldsymbol{v} - \boldsymbol{v}_h^c) d\boldsymbol{s} \\
&= T_1 + T_2.
\end{aligned}$$

Cauchy–Schwarz inequality and (39), lead to

$$\begin{aligned}
T_1 &\lesssim \Big(\nu^{-1} \sum_{K \in \mathscr{T}_h} h_K^2 \|\lambda_h \boldsymbol{u}_h + \nu \Delta \boldsymbol{u}_h - \nabla p_h\|_{0,K}^2\Big)^{1/2} \Big(\nu \sum_{K \in \mathscr{T}_h} h_K^{-2} \|\boldsymbol{v} - \boldsymbol{v}_h^c\|_{0,K}^2\Big)^{1/2} \\
&\lesssim \Big(\sum_{K \in \mathscr{T}_h} \eta_{R_K}^2\Big)^{1/2} |||\boldsymbol{v}|||.
\end{aligned}$$

Since $(\boldsymbol{v} - \boldsymbol{v}_h^c)|_{\partial\Omega} = 0$ we can rewrite T_2 in terms of a sum over interior edges

$$T_2 = \sum_{E \in \mathscr{E}_h^i} \int_E [\![(p_h \boldsymbol{I} - \nu \nabla \boldsymbol{u}_h)\boldsymbol{n}]\!] (\boldsymbol{v} - \boldsymbol{v}_h^c) d\boldsymbol{s}.$$

Again, applying Cauchy–Schwarz inequality and (39), imply

$$\begin{aligned}
T_2 &\lesssim \Big(\nu^{-1} \sum_{E \in \mathscr{E}_h^i} h_E \|[\![(p_h \boldsymbol{I} - \nu \nabla \boldsymbol{u}_h)\boldsymbol{n}]\!]\|_{0,E}^2\Big)^{1/2} \Big(\nu \sum_{E \in \mathscr{E}_h^i} h_E^{-1} \|\boldsymbol{v} - \boldsymbol{v}_h^c\|_{0,E}^2\Big)^{1/2} \\
&\lesssim \Big(\sum_{K \in \mathscr{T}_h} \eta_{E_K}^2\Big)^{1/2} |||\boldsymbol{v}|||.
\end{aligned}$$

Combining the above estimates, proves the desired result. □

Lemma 5 *Let $(\boldsymbol{u}, p, \lambda) \in \boldsymbol{H}_0^1(\Omega) \times L_0^2(\Omega) \times \mathbb{R}_+$ solve (3) and $(\boldsymbol{u}_h, p_h, \lambda_h) \in \boldsymbol{V}_h \times Q_h \times \mathbb{R}_+$ solve (6), then we have the following upper bound for the conforming velocity and pressure errors*

$$\left|\left|\left| \boldsymbol{u} - \boldsymbol{u}_h^c \right|\right|\right| + \nu^{-1/2} \|p - p_h\|_0 \lesssim \eta_h + \nu^{-1/2} \left(|\lambda - \lambda_h| + \lambda \|\boldsymbol{u} - \boldsymbol{u}_h\|_0\right).$$

Proof Using Lemma 2, there exists a pair $(\boldsymbol{v}, q) \in \boldsymbol{H}_0^1(\Omega) \setminus \{0\} \times L_0^2(\Omega)$ such that

$$\left|\!\left|\!\left|(\boldsymbol{u} - \boldsymbol{u}_h^c, p - p_h)\right|\!\right|\!\right|^2 \lesssim \mathscr{A}_h(\boldsymbol{u} - \boldsymbol{u}_h^c, p - p_h; \boldsymbol{v}, q),$$

and

$$|\!|\!|(\boldsymbol{v}, q)|\!|\!| \lesssim \left|\!\left|\!\left|(\boldsymbol{u} - \boldsymbol{u}_h^c, p - p_h)\right|\!\right|\!\right|.$$

Since $\boldsymbol{u}, \boldsymbol{u}_h^c, \boldsymbol{v} \in \boldsymbol{H}_0^1(\Omega)$, we have

$$\mathscr{A}_h(\boldsymbol{u} - \boldsymbol{u}_h^c, p - p_h; \boldsymbol{v}, q) = \nu(\nabla(\boldsymbol{u} - \boldsymbol{u}_h^c), \nabla \boldsymbol{v}) - (p - p_h, \nabla \cdot \boldsymbol{v}) - (q, \nabla \cdot (\boldsymbol{u} - \boldsymbol{u}_h^c)).$$

From (3), we obtain

$$\mathscr{A}_h(\boldsymbol{u} - \boldsymbol{u}_h^c, p - p_h; \boldsymbol{v}, q) = \lambda(\boldsymbol{u}, \boldsymbol{v}) - \nu(\nabla \boldsymbol{u}_h^c, \nabla \boldsymbol{v}) + (p_h, \nabla \cdot \boldsymbol{v}) + (q, \nabla \cdot \boldsymbol{u}_h^c).$$

Applying the fact $(q, \nabla \cdot \boldsymbol{u}_h) = 0$, implies

$$\begin{aligned} \mathscr{A}_h(\boldsymbol{u} - \boldsymbol{u}_h^c, p - p_h; \boldsymbol{v}, q) &= \lambda(\boldsymbol{u}, \boldsymbol{v}) - \nu(\nabla \boldsymbol{u}_h^c, \nabla \boldsymbol{v}) + (p_h, \nabla \cdot \boldsymbol{v}) - (q, \nabla \cdot \boldsymbol{u}_h^r) \\ &= \lambda_h(\boldsymbol{u}_h, \boldsymbol{v}) + (\lambda \boldsymbol{u} - \lambda_h \boldsymbol{u}_h, \boldsymbol{v}) - \nu(\nabla_h \boldsymbol{u}_h, \nabla \boldsymbol{v}) \\ &\quad + \nu(\nabla_h \boldsymbol{u}_h^r, \nabla \boldsymbol{v}) + (p_h, \nabla \cdot \boldsymbol{v}) - (q, \nabla \cdot \boldsymbol{u}_h^r). \end{aligned}$$

Let $\boldsymbol{v}_h^c = \boldsymbol{\Pi}_h \boldsymbol{v} \in \boldsymbol{V}_h^c$ be the Scott–Zhang interpolation of $\boldsymbol{v}$. Using (6) gives

$$0 = \lambda_h(\boldsymbol{u}_h, \boldsymbol{v}_h^c) - \nu(\nabla_h \boldsymbol{u}_h, \nabla \boldsymbol{v}_h^c) - C_h(\boldsymbol{u}_h, \boldsymbol{v}_h^c) + (p_h, \nabla \cdot \boldsymbol{v}_h^c).$$

Then we have

$$\mathscr{A}_h(\boldsymbol{u} - \boldsymbol{u}_h^c, p - p_h; \boldsymbol{v}, q) = T_1 + T_2 + T_3 + T_4,$$

where

$$\begin{aligned} &T_1 = \lambda_h(\boldsymbol{u}_h, \boldsymbol{v} - \boldsymbol{v}_h^c) - \nu(\nabla_h \boldsymbol{u}_h, \nabla(\boldsymbol{v} - \boldsymbol{v}_h^c)) + (p_h, \nabla \cdot (\boldsymbol{v} - \boldsymbol{v}_h^c)), \\ &T_2 = \nu(\nabla_h \boldsymbol{u}_h^r, \nabla \boldsymbol{v}) - (q, \nabla \cdot \boldsymbol{u}_h^r), \quad T_3 = C_h(\boldsymbol{u}_h, \boldsymbol{v}_h^c), \quad T_4 = (\lambda \boldsymbol{u} - \lambda_h \boldsymbol{u}_h, \boldsymbol{v}). \end{aligned}$$

Using Lemma 4, we have

$$T_1 \lesssim \eta_h |\!|\!|\boldsymbol{v}|\!|\!|.$$

Cauchy–Schwarz inequality and (36) show

$$T_2 \lesssim \left|\!\left|\!\left|\boldsymbol{u}_h^r\right|\!\right|\!\right| |\!|\!|(\boldsymbol{v}, q)|\!|\!| \lesssim \eta_h |\!|\!|(\boldsymbol{v}, q)|\!|\!|.$$

Using Lemma 3 for the bound of T_3, we have

$$T_3 \lesssim \gamma^{-1/2} \eta_h |||\boldsymbol{v}|||.$$

Cauchy–Schwarz and Poincare inequality lead to

$$T_4 \lesssim \nu^{-1/2} \|\lambda \boldsymbol{u} - \lambda_h \boldsymbol{u}_h\|_0 |||\boldsymbol{v}||| \lesssim \nu^{-1/2} \left(|\lambda - \lambda_h| + \lambda \|\boldsymbol{u} - \boldsymbol{u}_h\|_0 \right) |||\boldsymbol{v}|||.$$

Combining the above with the estimate $|||(\boldsymbol{v}, q)||| \lesssim \left|\left|\left|(\boldsymbol{u} - \boldsymbol{u}_h^c, p - p_h)\right|\right|\right|$ yields the desired result. □

Theorem 5 *Let* $(\boldsymbol{u}, p, \lambda) \in \boldsymbol{H}_0^1(\Omega) \times L_0^2(\Omega) \times \mathbb{R}_+$ *be the solution of the Stokes eigenvalue problem* (3) *and* $(\boldsymbol{u}_h, p_h, \lambda_h) \in \boldsymbol{V}_h \times Q_h$ *the* H^{div}*-DG approximation obtained by* (6). *Let* η_h *be the a posteriori error estimator in* (31). *Then we obtain the following a posteriori error bound*

$$|||\boldsymbol{u} - \boldsymbol{u}_h||| + \nu^{-1/2} \|p - p_h\|_0 \lesssim \eta_h + \nu^{-1/2} \left(|\lambda - \lambda_h| + \lambda \|\boldsymbol{u} - \boldsymbol{u}_h\|_0 \right),$$

where the hidden constant is independent of the sufficiently large penalty parameter $\gamma \geq 1$.

Proof The proof follows directly from a combination of Lemma 5 and (36). □

Theorem 6 *If* $\boldsymbol{u} \in \boldsymbol{H}^2(\mathscr{T}_h)$ *and* $p \in H^1(\mathscr{T}_h)$, *then the eigenvalue error satisfies*

$$|\lambda - \lambda_h| \lesssim \eta_h^2 + \nu^{-1} |\lambda - \lambda_h|^2 + (\lambda + \nu^{-1}\lambda^2) \|\boldsymbol{u} - \boldsymbol{u}_h\|_0^2 + |C_h(\boldsymbol{u} - \boldsymbol{u}_h, \boldsymbol{u} - \boldsymbol{u}_h)|,$$

where the hidden constant is independent of the sufficiently large penalty parameter $\gamma \geq 1$.

Proof Note that since $\nabla \cdot \boldsymbol{u} = 0 = \nabla \cdot \boldsymbol{u}_h$, we have

$$\begin{aligned}\mathscr{A}_h(\boldsymbol{u} - \boldsymbol{u}_h, p - p_h; \boldsymbol{u} - \boldsymbol{u}_h, p - p_h) &= a_h(\boldsymbol{u} - \boldsymbol{u}_h, \boldsymbol{u} - \boldsymbol{u}_h) \\ &= |||\boldsymbol{u} - \boldsymbol{u}_h|||^2 + C_h(\boldsymbol{u} - \boldsymbol{u}_h, \boldsymbol{u} - \boldsymbol{u}_h).\end{aligned}$$

The assertion then follows from a combination of the above with Theorems 4 and 5. □

Remark 4 From the estimates in [35, Proposition 8.1], we can conclude that the consistency error $|C_h(\boldsymbol{u} - \boldsymbol{u}_h, \boldsymbol{u} - \boldsymbol{u}_h)|$, with $C_h(\cdot, \cdot)$ from (38), is of the same order as $|\lambda - \lambda_h|$. However, we observe in all the experiments of Sect. 5 that η_h^2 provides a reliable bound of the eigenvalue error even on very coarse meshes. Hence, it is empirically justified to neglect the consistency error in the a posteriori error estimator.

4.3 Efficiency

This section is devoted to prove an efficiency bound for η. To prove the results, we use the bubble function technique which was introduced in [39,40].

Let K be an element of $\mathscr{T}_h$. We consider the standard element bubble function b_K on K. Let $\boldsymbol{v}_h$ be any vector valued polynomial function on K, then the following results hold from [1,26,39],

$$\begin{aligned} \|\boldsymbol{v}_h\|_{0,K} &\lesssim \|b_K^{1/2}\boldsymbol{v}_h\|_{0,K}, \\ \|b_K\boldsymbol{v}_h\|_{0,K} &\lesssim \|\boldsymbol{v}_h\|_{0,K}, \\ \|\nabla(b_K\boldsymbol{v}_h)\|_{0,K} &\lesssim h_K^{-1}\|\boldsymbol{v}_h\|_{0,K}. \end{aligned} \tag{40}$$

Lemma 6 *For $\boldsymbol{u}_h \in \boldsymbol{V}_h$, it holds that*

$$\left(\sum_{K\in\mathscr{T}_h} \eta_{J_K}^2\right)^{1/2} \lesssim |||\boldsymbol{u}-\boldsymbol{u}_h|||.$$

Proof Using $[\![\boldsymbol{u}\otimes\boldsymbol{n}]\!]=0$, we get

$$\eta_{J_K}^2 = \nu\sum_{E\in\partial K}\gamma_h\|[\![\boldsymbol{u}_h\otimes\boldsymbol{n}]\!]\|_{0,E}^2 = \nu\sum_{E\in\partial K}\gamma_h\|[\![(\boldsymbol{u}_h-\boldsymbol{u})\otimes\boldsymbol{n}]\!]\|_{0,E}^2.$$

Summing over all $K\in\mathscr{T}_h$, we have

$$\left(\sum_{K\in\mathscr{T}_h}\eta_{J_K}^2\right)^{1/2} \lesssim \left(\nu\sum_{E\in\mathscr{E}_h}\gamma_h\|[\![(\boldsymbol{u}_h-\boldsymbol{u})\otimes\boldsymbol{n}]\!]\|_{0,E}^2\right)^{1/2} \lesssim |||\boldsymbol{u}-\boldsymbol{u}_h|||.$$

□

Lemma 7 *Let $(\boldsymbol{u},p,\lambda)\in \boldsymbol{H}_0^1(\Omega)\times L_0^2(\Omega)\times\mathbb{R}_+$ solve (3), and $(\boldsymbol{u}_h,p_h,\lambda_h)\in\boldsymbol{V}_h\times Q_h\times\mathbb{R}_+$. Then we have*

$$\begin{aligned} \left(\sum_{K\in\mathscr{T}_h}\eta_{R_K}^2\right)^{1/2} &= \left(\sum_{K\in\mathscr{T}_h}\nu^{-1}h_K^2\|\lambda_h\boldsymbol{u}_h+\nu\Delta\boldsymbol{u}_h-\nabla p_h\|_{0,K}^2\right)^{1/2} \\ &\lesssim |||\boldsymbol{u}-\boldsymbol{u}_h|||+\nu^{-1/2}\|p-p_h\|+h.o.t., \end{aligned}$$

where $h.o.t. = \nu^{-1/2}\left(\sum_{K\in\mathscr{T}_h}h_K^2\|\lambda\boldsymbol{u}-\lambda_h\boldsymbol{u}_h\|_{0,K}^2\right)^{1/2}.$

Proof Define the functions R and W locally for any $K\in\mathscr{T}_h$ by

$$R|_K = \lambda_h\boldsymbol{u}_h+\nu\Delta\boldsymbol{u}_h-\nabla p_h \quad\text{and}\quad W|_K=\nu^{-1}h_K^2Rb_K.$$

From (40) we have

$$\begin{aligned}\eta_{R_K}^2 &= \nu^{-1}h_K^2\|R\|_{0,K}^2 \lesssim \int_K R\cdot(\nu^{-1}h_K^2 R b_K)d\boldsymbol{x}\\ &= \int_K(\lambda_h\boldsymbol{u}_h + \nu\Delta\boldsymbol{u}_h - \nabla p_h)\cdot W\,d\boldsymbol{x}.\end{aligned}$$

Note that $\lambda\boldsymbol{u} + \nu\Delta\boldsymbol{u} - \nabla p = 0$. Subtracting this from the last term, using integration by parts and $W|_{\partial K} = 0$, we obtain

$$\eta_{R_K}^2 \lesssim \nu\int_K \nabla(\boldsymbol{u}-\boldsymbol{u}_h)\cdot\nabla W\,d\boldsymbol{x} + \int_K (p_h - p)\nabla\cdot W\,d\boldsymbol{x} + \int_K(\lambda_h\boldsymbol{u}_h - \lambda\boldsymbol{u})\cdot W\,d\boldsymbol{x}.$$

Applying Cauchy–Schwarz inequality, implies

$$\begin{aligned}\eta_{R_K}^2 \lesssim &\left(\nu^{1/2}\|\nabla(\boldsymbol{u}-\boldsymbol{u}_h)\|_{0,K} + \nu^{-1/2}\|p-p_h\|_{0,K} + \nu^{-1/2}h_K\|\lambda_h\boldsymbol{u}_h - \lambda\boldsymbol{u}\|_{0,K}\right)\\ &\left(\nu^{1/2}\|\nabla W\|_{0,K} + \nu^{1/2}h_K^{-1}\|W\|_{0,K}\right).\end{aligned} \tag{41}$$

From (40) we get

$$\nu^{1/2}\|\nabla W\|_{0,K} + \nu^{1/2}h_K^{-1}\|W\|_{0,K} \lesssim \nu^{-1/2}h_K\|R\|_{0,K} = \eta_{R_K}.$$

Hence, dividing (41) by η_{R_K} and taking the square-root of the sum of the squares over all $K \in \mathscr{T}_h$ ends the proof. □

Let E be an interior edge which is shared by two elements K_1 and K_2. Let b_E denote the standard polynomial edge bubble function for E with support in $\omega_E = \{K_1, K_2\}$. In case of a regular edge E, we choose $\widetilde{K} = K_2$. When one vertex of E is a hanging node, then we choose K_1 such that E is an entire edge of K_1 and define $\widetilde{K} \subset K_2$ as the largest rectangle contained in K_2 such that E is one of the entire edges of $\widetilde{K}$. We then set $\widetilde{\omega}_E = \{K, \widetilde{K}\}$.

If $\boldsymbol{\sigma}$ is a vector-valued polynomial function on E, then

$$\|\boldsymbol{\sigma}\|_{0,E} \lesssim \|b_E^{1/2}\boldsymbol{\sigma}\|_{0,E}. \tag{42}$$

Moreover we can define an extension $\boldsymbol{\sigma}_b \in \boldsymbol{H}_0^1(\widetilde{\omega}_E)$ such that $\boldsymbol{\sigma}_b|_E = b_E\boldsymbol{\sigma}$ and from [1,26,39] we have

$$\begin{aligned}\|\boldsymbol{\sigma}_b\|_{0,K} &\lesssim h_E^{1/2}\|\boldsymbol{\sigma}\|_{0,E} \quad \forall K \in \widetilde{\omega}_E,\\ \|\nabla\boldsymbol{\sigma}_b\|_{0,K} &\lesssim h_E^{-1/2}\|\boldsymbol{\sigma}\|_{0,E} \quad \forall K \in \widetilde{\omega}_E.\end{aligned} \tag{43}$$

Lemma 8 *Let* $(\boldsymbol{u}, p, \lambda) \in \boldsymbol{H}_0^1(\Omega) \times L_0^2(\Omega) \times \mathbb{R}_+$ *solve* (3)*, and* $(\boldsymbol{u}_h, p_h, \lambda_h) \in \boldsymbol{V}_h \times Q_h \times \mathbb{R}_+$*. Then we have*

$$\left(\sum_{K\in\mathscr{T}_h} \eta_{E_K}^2\right)^{1/2} = \left(\sum_{K\in\mathscr{T}_h} \nu^{-1} \sum_{E\in\partial K\setminus\partial\Omega} h_E \|[\![(p_h \boldsymbol{I} - \nu\nabla\boldsymbol{u}_h)\boldsymbol{n}]\!]\|_{0,E}^2\right)^{1/2}$$
$$\lesssim |||\boldsymbol{u}-\boldsymbol{u}_h||| + \nu^{-1/2}\|p - p_h\| + h.o.t.,$$

where $h.o.t. = \nu^{-1/2}\left(\sum_{K\in\mathscr{T}_h} h_K^2 \|\lambda\boldsymbol{u} - \lambda_h\boldsymbol{u}_h\|_{0,K}^2\right)^{1/2}.$

Proof Let for any interior edge $E \in \mathscr{E}_h^i$ the functions R and Λ be such that

$$R|_E = [\![(p_h\boldsymbol{I} - \nu\nabla\boldsymbol{u}_h)\boldsymbol{n}]\!]|_E \qquad \text{and} \qquad \Lambda = \nu^{-1}h_E R b_E.$$

Using (42) and $[\![(p\boldsymbol{I} - \nu\nabla\boldsymbol{u})\boldsymbol{n}]\!]|_E = 0$ we get

$$\nu^{-1}h_E\|R\|_{0,E}^2 \lesssim \int_E R\cdot(\nu^{-1}h_E R b_E)d\boldsymbol{s} = \int_E [\![((p_h - p)\boldsymbol{I} - \nu\nabla(\boldsymbol{u}_h - \boldsymbol{u}))\boldsymbol{n}]\!]\cdot\Lambda\, d\boldsymbol{s}$$

Using Green's formula over each of the two elements of $\tilde{\omega}_E$, gives

$$\begin{aligned}&\int_E [\![((p_h - p)\boldsymbol{I} - \nu\nabla(\boldsymbol{u}_h - \boldsymbol{u}))\boldsymbol{n}]\!]\cdot\Lambda\, d\boldsymbol{s}\\ &= \sum_{K\in\widetilde{\omega}_E}\int_K(-\nu\Delta(\boldsymbol{u}-\boldsymbol{u}_h) + \nabla(p-p_h))\cdot\Lambda\, d\boldsymbol{x}\\ &\quad - \sum_{K\in\widetilde{\omega}_E}\int_K(\nu\nabla(\boldsymbol{u}-\boldsymbol{u}_h) - (p-p_h)\boldsymbol{I}):\nabla\Lambda\, d\boldsymbol{x}.\end{aligned}$$

Using $\lambda\boldsymbol{u} + \nu\Delta\boldsymbol{u} - \nabla p = 0$, we obtain

$$\begin{aligned}\nu^{-1}h_E\|R\|_{0,E}^2 &\lesssim \sum_{K\in\widetilde{\omega}_E}\int_K(\lambda_h\boldsymbol{u}_h + \nu\Delta\boldsymbol{u}_h - \nabla p_h)\cdot\Lambda\, d\boldsymbol{x}\\ &\quad + \sum_{K\in\widetilde{\omega}_E}\int_K(\lambda\boldsymbol{u} - \lambda_h\boldsymbol{u}_h)\cdot\Lambda\, d\boldsymbol{x}\\ &\quad + \sum_{K\in\widetilde{\omega}_E}\int_K(-\nu\nabla(\boldsymbol{u}-\boldsymbol{u}_h) + (p-p_h)\boldsymbol{I}):\nabla\Lambda\, d\boldsymbol{x}\\ &= T_1 + T_2 + T_3.\end{aligned} \tag{44}$$

Using Cauchy–Schwarz inequality, shape-regularity of the mesh, and (43) yields

$$T_1 \lesssim \left(\sum_{K\in\widetilde{\omega}_E} \eta_{R_K}^2\right)^{1/2} \left(\sum_{K\in\widetilde{\omega}_E} \nu h_K^{-2}\|\Lambda\|_{0,K}^2\right)^{1/2} \lesssim \left(\sum_{K\in\widetilde{\omega}_E} \eta_{R_K}^2\right)^{1/2} \nu^{-1/2} h_E^{1/2}\|R\|_{0,E},$$

$$T_2 \lesssim \left(\sum_{K\in\widetilde{\omega}_E} \left(\nu^{-1} h_K^2\|\lambda \boldsymbol{u} - \lambda_h \boldsymbol{u}_h\|_{0,K}^2\right)\right)^{1/2} \nu^{-1/2} h_E^{1/2}\|R\|_{0,E},$$

as well as

$$T_3 \lesssim \left(\sum_{K\in\widetilde{\omega}_E} \left(\nu\|\nabla(\boldsymbol{u}-\boldsymbol{u}_h)\|_{0,K}^2 + \nu^{-1}\|p-p_h\|_{0,K}^2\right)\right)^{1/2} \nu^{-1/2} h_E^{1/2}\|R\|_{0,E}.$$

Combining the above estimates T_1, T_2 and T_3, dividing (44) by $\nu^{-1/2}h_E^{1/2}\|R\|_{0,E}$ and summing over all interior edges of all $K \in \mathscr{T}_h$, the desired result is proven by the finite overlap of the patches $\widetilde{\omega}_E$ and Lemma 7. □

Theorem 7 *Let $(\boldsymbol{u}, p, \lambda) \in \boldsymbol{H}_0^1(\Omega) \times L_0^2(\Omega) \times \mathbb{R}_+$ be the solution of the Stokes eigenvalue problem (3) and $(\boldsymbol{u}_h, p_h, \lambda_h) \in \boldsymbol{V}_h \times Q_h \times \mathbb{R}_+$ the H^{div}-DG approximation obtained by (6). Then the a posteriori error estimator η_h is efficient in the sense that*

$$\eta_h \lesssim |||\boldsymbol{u}-\boldsymbol{u}_h||| + \nu^{-1/2}\|p-p_h\|_0 + h.o.t.$$

where $h.o.t. = \nu^{-1/2}\left(\sum_{K\in\mathscr{T}_h} h_K^2\|\lambda\boldsymbol{u}-\lambda_h\boldsymbol{u}_h\|_{0,K}^2\right)^{1/2}$.

Proof The statement follows from a combination of Lemmas 6–8. □

Theorem 8 *If $\boldsymbol{u} \in \boldsymbol{H}^2(\mathscr{T}_h)$ and $p \in H^1(\mathscr{T}_h)$, then the eigenvalue error satisfies*

$$\eta_h^2 \lesssim |\lambda-\lambda_h| + \nu^{-1}\|p-p_h\|_0^2 + \lambda\|\boldsymbol{u}-\boldsymbol{u}_h\|_0^2 + |C_h(\boldsymbol{u}-\boldsymbol{u}_h, \boldsymbol{u}-\boldsymbol{u}_h)| + (h.o.t.)^2,$$

where $h.o.t. = \nu^{-1/2}\left(\sum_{K\in\mathscr{T}_h} h_K^2\|\lambda\boldsymbol{u}-\lambda_h\boldsymbol{u}_h\|_{0,K}^2\right)^{1/2}$*, and C_h is as defined in (38).*

Proof From Theorem 7, we deduce

$$\eta_h^2 \lesssim |||\boldsymbol{u}-\boldsymbol{u}_h|||^2 + \nu^{-1}\|p-p_h\|_0^2 + (h.o.t.)^2. \tag{45}$$

Since $\nabla\cdot\boldsymbol{u} = 0 = \nabla\cdot\boldsymbol{u}_h$, we have

$$\begin{aligned}\mathscr{A}_h(\boldsymbol{u}-\boldsymbol{u}_h, p-p_h; \boldsymbol{u}-\boldsymbol{u}_h, p-p_h) &= a_h(\boldsymbol{u}-\boldsymbol{u}_h, \boldsymbol{u}-\boldsymbol{u}_h)\\ &= |||\boldsymbol{u}-\boldsymbol{u}_h|||^2 + C_h(\boldsymbol{u}-\boldsymbol{u}_h, \boldsymbol{u}-\boldsymbol{u}_h).\end{aligned}$$

Therefore, Theorem 4 shows

$$|||\boldsymbol{u}-\boldsymbol{u}_h|||^2 = \lambda_h - \lambda + \lambda\|\boldsymbol{u}-\boldsymbol{u}_h\|_0^2 - C_h(\boldsymbol{u}-\boldsymbol{u}_h, \boldsymbol{u}-\boldsymbol{u}_h). \tag{46}$$

Combining (45) and (46) implies the result. □

Remark 5 From the estimates in [35, Proposition 8.1], the eigenvalue estimate (22), and the pressure estimate (28), we can conclude that $\nu^{-1}\|p-p_h\|_0^2+|C_h(\boldsymbol{u}-\boldsymbol{u}_h, \boldsymbol{u}-\boldsymbol{u}_h)|$ is of the same order as $|\lambda-\lambda_h|$. Moreover, from Remark 3 we see that the unfavorable factor ν^{-1} in front of the pressure error is compensated by the scaling of the pressure p by a factor ν.

5 Numerical experiments

This section is devoted to several numerical experiments on one convex and two non-convex domains. The experiments verify reliability and efficiency of the proposed a posteriori error estimator of Sect. 4 for the eigenvalue error of (simple) eigenvalues and up to polynomial degree 3.

We employ the standard adaptive finite element loop with the steps *solve*, *estimate*, *mark* and *refine*. To solve the algebraic eigenvalue problem we use the ARPACK library [30] in combination with a direct solver. We mark elements of the mesh for refinement on the level ℓ in a minimal set $\mathscr{M}_\ell$ using the bulk marking strategy [15] with bulk parameter $\theta = 1/2$, i.e. $\mathscr{M}_\ell$ is the minimal set such that $\theta\sum_{K\in\mathscr{T}_\ell}\eta_K^2 \le \sum_{K\in\mathscr{M}_\ell}\eta_K^2$. The mesh is refined with one level irregular nodes. The implementation of the method is done in the software library amandus [24], which is based on the dealii finite element library [5].

In all experiments we chose the penalty parameter $\gamma = k(k+1)/2$ for k-th order $RT_k \times Q_k$ finite element pairs, $k = 1, 2, 3$. Since the eigenvalues of the Stokes problem are related to the eigenvalues of the buckling eigenvalue problem of clamped plates via the stream function formulation, we can use reference values for the eigenvalues from [6,10,37].

5.1 Square domain

In this example, we consider the square domain $\Omega = (0, 1)^2$. The reference value for the first eigenvalue reads $\lambda_1 = 52.344691168$ [6,10,37]. The streamline plot of the discrete eigenfunction $\boldsymbol{u}_\ell$ and the plot of the discrete pressure p_ℓ on a uniform mesh for $\nu = 1$, $k = 1$ are displayed in Fig. 1a, b, respectively.

First we confirm that the presented a posteriori error estimator is in practice robust in ν, which is due to the scaling of the pressure, cf. Remark 3. Table 1 shows perfectly constant efficiency indices $\frac{\eta_h^2}{|\lambda-\lambda_\ell|}$ for varying ν and $k = 1$. Hence, there is no need to

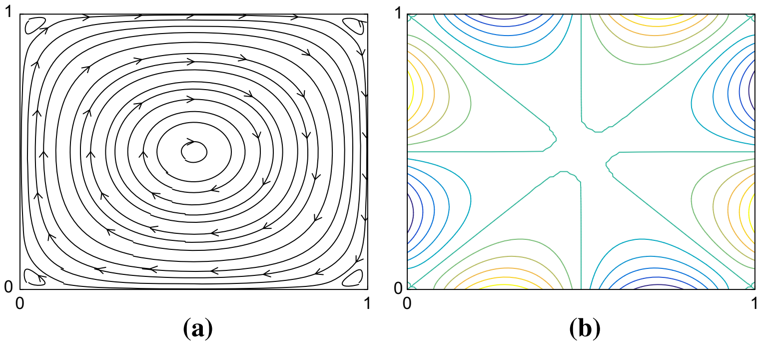

Fig. 1 Streamline plot of the discrete eigenfunction $\boldsymbol{u}_\ell$ (**a**), and plot of the discrete pressure p_ℓ (**b**)

Table 1 Efficiency indices for different ν, $k = 1$, and uniform meshes

ℓ	$\nu = 10$	$\nu = 1$	$\nu = 10^{-1}$	$\nu = 10^{-2}$	$\nu = 10^{-3}$	$\nu = 10^{-4}$
1	31.0416	31.0416	31.0416	31.0416	31.0416	31.0416
2	26.6298	26.6298	26.6298	26.6298	26.6298	26.6298
3	25.1283	25.1283	25.1283	25.1283	25.1283	25.1283
4	24.5267	24.5267	24.5267	24.5267	24.5267	24.5267
5	24.2555	24.2555	24.2555	24.2555	24.2555	24.2555
6	24.1267	24.1267	24.1267	24.1267	24.1267	24.1267

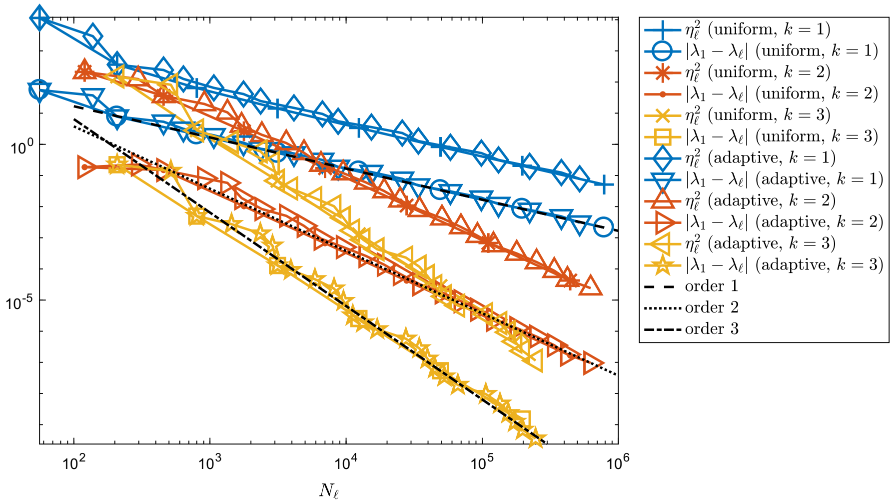

Fig. 2 Convergence history of $|\lambda_1 - \lambda_\ell|$ and η_ℓ^2 on uniformly and adaptively refined meshes for the square domain

consider the pressure-robust estimators of [27,29] for the Stokes eigenvalue problem, and from now on we may set $\nu = 1$. Note that the efficiency indices for the eigenvalues are related to the square-root of the efficiency indices for the eigenfunctions. Therefore

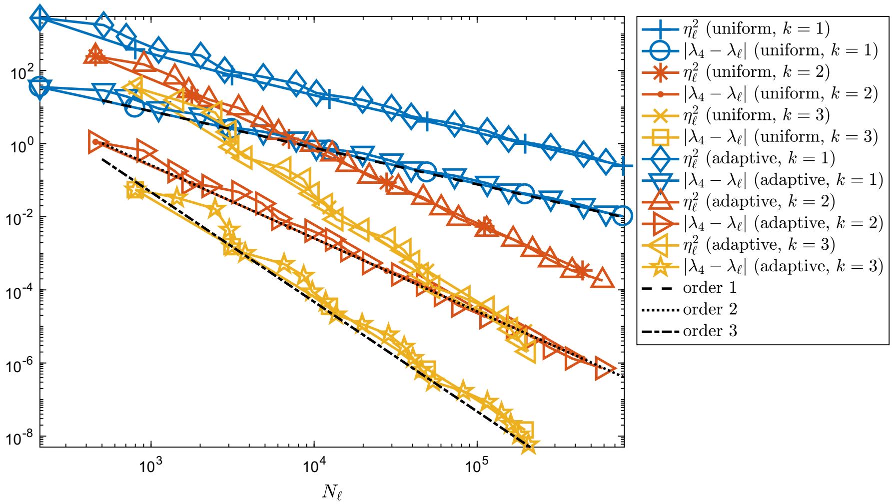

Fig. 3 Convergence history of $|\lambda_4 - \lambda_\ell|$ and η_ℓ^2 on uniformly and adaptively refined meshes for the square domain

the value 25 relates to the value 5 for the eigenfunction error which is in the typical range of efficiency indices for residual based a posteriori error estimators for the source problem.

In Fig. 2, we observe that both uniform and adaptive mesh refinement leads to optimal orders of convergence $\mathcal{O}(N_\ell^{-k})$ for the eigenvalue error $|\lambda_1 - \lambda_\ell|$. This is due to the fact that the domain is convex and the first eigenfunction is smooth enough. Note that for uniform meshes $\mathcal{O}(N_\ell^{-k}) \approx \mathcal{O}(h^{2k})$, for $N_\ell = \dim(V_h \times Q_h)$. We observe that the convergence graphs for uniform and adaptive mesh refinement overlap each other for both the eigenvalue errors $|\lambda_1 - \lambda_\ell|$ as well the a posteriori error estimators η_ℓ^2. Moreover, we confirm that the a posteriori error estimator η_ℓ^2 is numerically reliable and efficient.

The reference value for the fourth eigenvalue, which is simple, reads $\lambda_4 \approx 128.209584313$. In Fig. 3 we observe the same behavior of η_ℓ^2 for the fourth eigenvalue as in Fig. 2 for the first eigenvalue, namely both uniform and adaptive mesh refinement lead to optimal convergence and the a posteriori error estimator shows to be reliable and efficient.

5.2 L-shaped domain

In the second example, we take the non-convex L-shaped domain $\Omega = (-1, 1)^2 \backslash (0, 1)^2$ with a re-entrant corner at the origin, which allows for singular eigenfunctions.

To compute the error of the first eigenvalue, we take $\lambda = 32.13269465$ as a reference value from [16]. Figure 4a, b show the computed velocity and discrete pressure as a streamline plot on a uniform mesh computed with $k = 1$. The exponent for the singular function at the re-entrant corner is known to be $\alpha \approx 0.544483736782464$. Hence, in Fig. 5 we observe suboptimal convergence of $\mathcal{O}(N_\ell^{-0.544})$ for the eigenvalue error even

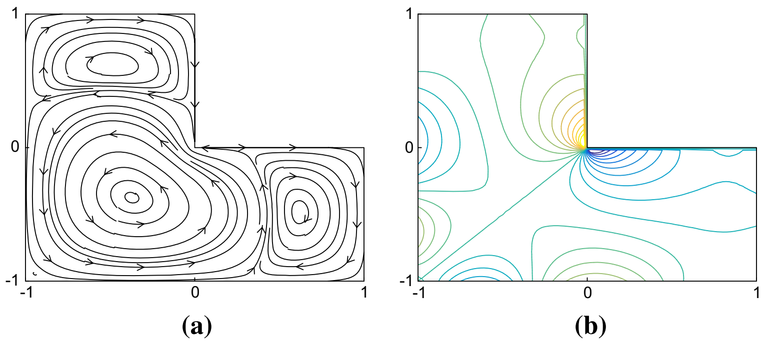

Fig. 4 Streamline plot of the discrete eigenfunction $\boldsymbol{u}_\ell$ (**a**), and plot of the of discrete pressure p_ℓ (**b**)

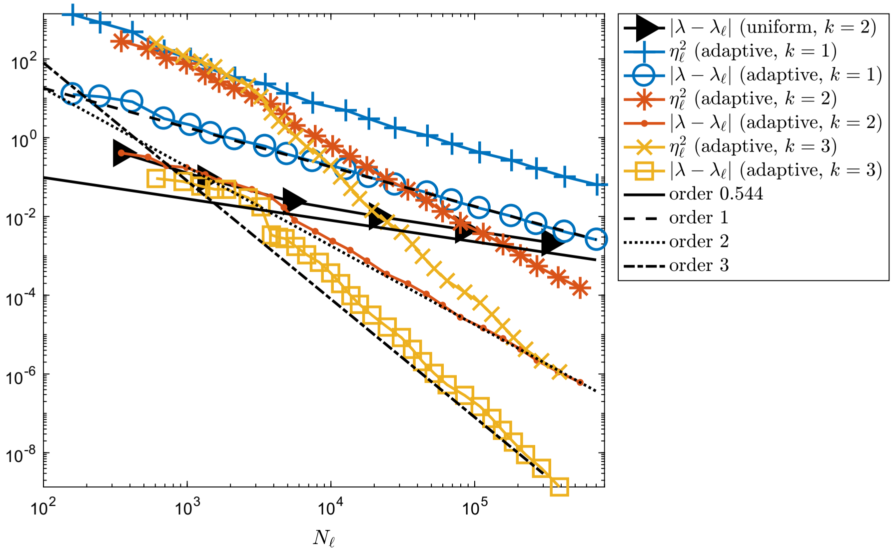

Fig. 5 Convergence history of $|\lambda - \lambda_\ell|$ and η_ℓ^2 on uniformly and adaptively refined meshes for the L-shaped domain

for $k = 2$. Adaptive mesh refinement however, achieves optimal convergence $\mathcal{O}(N_\ell^{-k})$ of the eigenvalue error for $k = 1, 2, 3$. The a posteriori error estimator η_ℓ^2 shows to be reliable and efficient in all experiments. Observe that the eigenvalue error obtained with $k = 3$ on adaptively refined meshes is about 6 orders of magnitude smaller than that for uniform mesh refinement. This demonstrates the importance of mesh adaptivity, in particular for high order methods. Figure 6a–c show some adaptively refined meshes for $k = 1, 2, 3$, which show strong refinement towards the origin.

5.3 Slit domain

In the last example, let $\Omega = (-1, 1)^2 \backslash (\{0\} \times (-1, 0))$ be the slit domain. To compute the error of the first eigenvalue, we take $\lambda = 29.9168629$ as a reference value from [16].

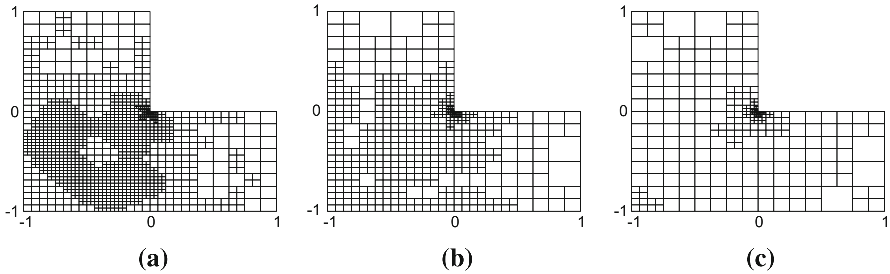

Fig. 6 Adaptively refined meshes for $RT_1 \times Q_1$ (**a**), $RT_2 \times Q_2$ (**b**), and $RT_3 \times Q_3$ (**c**)

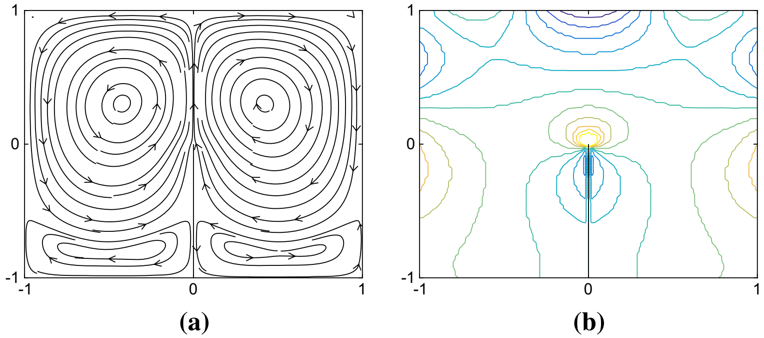

Fig. 7 Streamline plot of the discrete eigenfunction $\boldsymbol{u}_\ell$ (**a**), and plot of the discrete pressure p_ℓ (**b**)

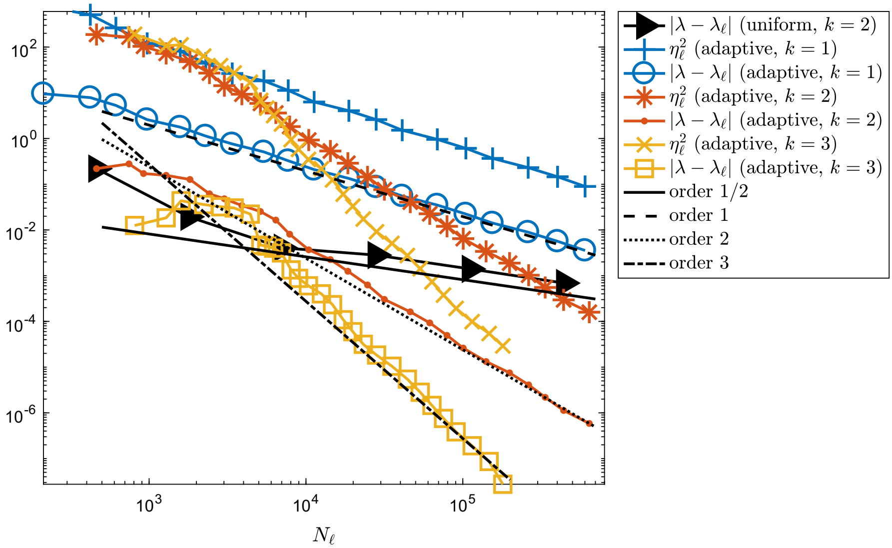

Fig. 8 Convergence history of $|\lambda - \lambda_\ell|$ and η_ℓ^2 on uniformly and adaptively refined meshes for the slit domain

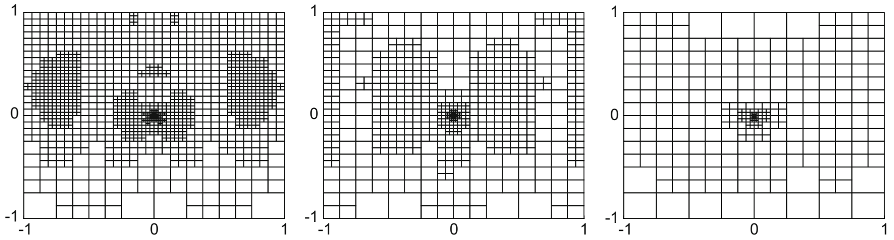

Fig. 9 Adaptively refined meshes for $RT_1 \times Q_1$ (**a**), $RT_2 \times Q_2$ (**b**), and $RT_3 \times Q_3$ (**c**)

The discrete velocity eigenfunction $\boldsymbol{u}_\ell$ and discrete pressure p_ℓ are displayed in Fig. 7a, b as a streamline plot on a uniform mesh for $k = 1$. In Fig. 8, we observe suboptimal convergence of $\mathcal{O}(N_\ell^{-1/2})$ for the eigenvalue error on uniform meshes, but optimal convergence of $\mathcal{O}(N_\ell^{-k})$ for $k = 1, 2, 3$, for adaptively refined meshes. Moreover, the a posteriori error estimator proves to be numerically reliable and efficient. Note that we had to stop the third order method on adaptively refined meshes earlier than for the lower order methods, since the accuracy of the reference value has been already reached with less than $2 \cdot 10^5$ degrees of freedom. Figure 9a–c show some adaptively refined meshes for $k = 1, 2, 3$, which are strongly refined towards the tip of the slit at the origin.

Acknowledgements The authors would like to thank the two anonymous referees for their valuable suggestions that lead to an improvement of this article.

References

1. Ainsworth, M., Oden, J.T.: A Posteriori Error Estimation in Finite Element Analysis (Pure and Applied Mathematics). Wiley, New York (2000)
2. Armentano, M.G., Moreno, V.: A posteriori error estimates of stabilized low-order mixed finite elements for the Stokes eigenvalue problem. J. Comput. Appl. Math. **269**, 132–149 (2014)
3. Arnold, D.N.: An interior penalty finite element method with discontinuous elements. SIAM J. Numer. Anal. **19**(4), 742–760 (1982)
4. Babuška, I., Osborn, J.: Eigenvalue problems. In: Handbook of Numerical Analysis, Vol. II, Handb. Numer. Anal., II, pp. 641–787. North-Holland, Amsterdam (1991)
5. Bangerth, W., Davydov, D., Heister, T., Heltai, L., Kanschat, G., Kronbichler, M., Maier, M., Turcksin, B., Wells, D.: The deal.II library, version 8.4. J. Numer. Math. **24**(3), 135–141 (2016)
6. Bjørstad, P.E., Tjøstheim, B.P.: High precision solutions of two fourth order eigenvalue problems. Computing **63**(2), 97–107 (1999)
7. Boffi, D.: Finite element approximation of eigenvalue problems. Acta Numer. **19**, 1–120 (2010)

8. Boffi, D., Gallistl, D., Gardini, F., Gastaldi, L.: Optimal convergence of adaptive FEM for eigenvalue clusters in mixed form. Math. Comput. **86**(307), 2213–2237 (2017)
9. Boyer, F., Fabrie, P.: Mathematical Tools for the Study of the Incompressible Navier–Stokes Equations and Related Models (Applied Mathematical Sciences), vol. 183. Springer, New York (2013). https://doi.org/10.1007/978-1-4614-5975-0
10. Brenner, S.C., Monk, P., Sun, J.: C^0 interior penalty Galerkin method for biharmonic eigenvalue problems. In: Spectral and High Order Methods for Partial Differential Equations—ICOSAHOM 2014, Lecture Notes in Computational Science and Engineering, vol. 106, pp. 3–15. Springer, Cham (2015)
11. Brezzi, F., Douglas, J., Marini, L.D.: Two families of mixed finite elements for second order elliptic problems. Numerische Mathematik **47**(2), 217–235 (1985)
12. Brezzi, F., Fortin, M.: Mixed and Hybrid Finite Element Methods, Springer Series in Computational Mathematics, vol. 15. Springer, New York (1991)
13. Cockburn, B., Kanschat, G., Schötzau, D.: A locally conservative LDG method for the incompressible Navier-Stokes equations. Math. Comput. **74**(251), 1067–1095 (2005)
14. Cockburn, B., Kanschat, G., Schötzau, D.: A note on discontinuous Galerkin divergence-free solutions of the Navier–Stokes equations. J. Sci. Comput. **31**(1–2), 61–73 (2007)
15. Dörfler, W.: A convergent adaptive algorithm for Poisson's equation. SIAM J. Numer. Anal. **33**(3), 1106–1124 (1996)
16. Gedicke, J., Khan, A.: Arnold-Winther mixed finite elements for Stokes eigenvalue problems. SIAM J. Sci. Comput. **40**(5), A3449–A3469 (2018)
17. Girault, V., Kanschat, G., Rivière, B.: Error analysis for a monolithic discretization of coupled Darcy and Stokes problems. J. Numer. Math. **22**(2), 109–142 (2014)
18. Girault, V., Raviart, P.A.: Finite Element Methods for Navier–Stokes Equations, Springer Series in Computational Mathematics, vol. 5. Springer, Berlin (1986)
19. Han, J., Zhang, Z., Yang, Y.: A new adaptive mixed finite element method based on residual type a posterior error estimates for the Stokes eigenvalue problem. Numer. Methods Partial Differ. Equ. **31**(1), 31–53 (2015)
20. Houston, P., Schötzau, D., Wihler, T.P.: Energy norm a posteriori error estimation for mixed discontinuous Galerkin approximations of the Stokes problem. J. Sci. Comput. **22**(23), 347–370 (2005)
21. Huang, P.: Lower and upper bounds of Stokes eigenvalue problem based on stabilized finite element methods. Calcolo **52**(1), 109–121 (2015)
22. Huang, P., He, Y., Feng, X.: Numerical investigations on several stabilized finite element methods for the Stokes eigenvalue problem. Math. Probl. Eng. p. Art. ID 745908, 14 (2011)
23. John, V., Linke, A., Merdon, C., Neilan, M., Rebholz, L.G.: On the divergence constraint in mixed finite element methods for incompressible flows. SIAM Rev. **59**(3), 492–544 (2017)
24. Kanschat, G.: Amandus. https://bitbucket.org/guidokanschat/amandus. A simple experimentation suite built on the dealii library. Accessed 16 Sept 2019
25. Kanschat, G., Mao, Y.: Multigrid methods for H^{div}-conforming discontinuous Galerkin methods for the Stokes equations. J. Numer. Math. **23**(1), 51–66 (2015)
26. Kanschat, G., Schötzau, D.: Energy norm a posteriori error estimation for divergence-free discontinuous Galerkin approximations of the Navier–Stokes equations. Int. J. Numer. Methods Fluids **57**(9), 1093–1113 (2008)
27. Kanschat, G., Sharma, N.: Divergence-conforming discontinuous Galerkin methods and C^0 interior penalty methods. SIAM J. Numer. Anal. **52**(4), 1822–1842 (2014)
28. Kellogg, R.B., Osborn, J.E.: A regularity result for the Stokes problem in a convex polygon. J. Funct. Anal. **21**(4), 397–431 (1976)
29. Lederer, P.L., Merdon, C., Schöberl, J.: Refined a posteriori error estimation for classical and pressure-robust Stokes finite element methods. Numer. Math. **142**(3), 713–748 (2019)
30. Lehoucq, R., Sorensen, D., Yang, C.: ARPACK Users' Guide: Solution of Large-Scale Eigenvalue Problems with Implicitly Restarted Arnoldi Methods. SIAM, Philadelphia (1998)
31. Liu, H., Gong, W., Wang, S., Yan, N.: Superconvergence and a posteriori error estimates for the Stokes eigenvalue problems. BIT **53**(3), 665–687 (2013)
32. Lovadina, C., Lyly, M., Stenberg, R.: A posteriori estimates for the Stokes eigenvalue problem. Numer. Methods Partial Differ. Equ. **25**(1), 244–257 (2009)
33. Meddahi, S., Mora, D., Rodríguez, R.: A finite element analysis of a pseudostress formulation for the Stokes eigenvalue problem. IMA J. Numer. Anal. **35**(2), 749–766 (2015)

34. Mercier, B., Osborn, J., Rappaz, J., Raviart, P.A.: Eigenvalue approximation by mixed and hybrid methods. Math. Comput. **36**(154), 427–453 (1981)
35. Schötzau, D., Schwab, C., Toselli, A.: Mixed *hp*-DGFEM for incompressible flows. SIAM J. Numer. Anal. **40**(6), 2171–2194 (2002)
36. Scott, L.R., Zhang, S.: Finite element interpolation of nonsmooth functions satisfying boundary conditions. Math. Comput. **54**(190), 483–493 (1990)
37. Sun, J., Zhou, A.: Finite Element Methods for Eigenvalue Problems. Monographs and Research Notes in Mathematics. CRC Press, Boca Raton (2017)
38. Toselli, A.: *hp* discontinuous Galerkin approximations for the Stokes problem. Math. Models Methods Appl. Sci. **12**(11), 1565–1597 (2002)
39. Verfürth, R.: A posteriori error estimation and adaptive mesh-refinement techniques. In: Proceedings of the Fifth International Congress on Computational and Applied Mathematics (Leuven, 1992), vol. 50, pp. 67–83 (1994)
40. Verfürth, R.: A Review of a posteriori Error Estimation and Adaptive Mesh-refinement Techniques. Teubner, Leipzig (1996)